Published in “*Journal of Asian Earth Sciences*”, Volume 254, 15 September 2023, 105736

Mode and timing of the Early Cretaceous transgression in Iran: insights from the stratigraphic evidence of sea-level changes and geodynamic events

Fabrizio Berra[1], Vincenzo Randazzo[1], Andrea Zanchi[2], Maria Rose Petrizzo[1], Felix Schlagintweit[3], Stefano Zanchetta[2], Hamid Reza Javadi[4]

[1]Dipartimento di Scienze della Terra “Adito Desio”, Università degli Studi di Milano, Italy

[2]Dipartimento di Scienze dell’Ambiente e della Terra, Università degli Studi di Milano – Bicocca, Italy

[3]Lerchenauerstr. 167, D-80935 München, Germany

[4] Geological Survey of Iran, Tehran, Iran

Keywords: Cretaceous; Orbitolina limestone; Iran; facies analysis; stratigraphy

Abstract

The study of selected logs from the Central-Eastern Iran Microplate (CEIM; area of Arusan) and Sanandaj–Sirjan Zone (SSZ; areas of Esfahan east and Tiran) constrains timing and evolution of the Cretaceous successions, resting unconformably on older sediments or non-conformably on the metamorphic basement. The Cretaceous marine transgression occurred almost synchronously on a levelled topography, documenting a previous deep erosion. Above a basal siliciclastic unit, rudist- and orbitolinid-rich lower Aptian limestone (“Orbitolina Limestone”, Shak Kuh Formation, Taft Formation) were deposited. Later, the stratigraphic evolution of the three studied areas differentiates, documenting changes in the depositional environments, reflecting different subsidence rates. In the Tiran area, marls and cherty limestones covering shallow-water limestones record a deepening trend. A differentiation of depositional environment is observed at Arusan, where conglomerates to the west pass to basinal sandstone and marls to the east. Here, a Coniacian-Campanian reprise of the carbonate production (with skeletal limestones rich in rudists, ostreids, and abundant orbitoidids) is covered by cherty marls. In the Esfahan north area, glauconitic hardground marls covered by chert record important deepening during the early Cenomanian, followed by the reprise of shallow-water carbonate production (middle Cenomanian). The synchronous deposition of Aptian carbonate successions on large parts of the CEIM, SSZ and North-Iranian domains suggests a rapid regional transgression controlled by a sea-level rise. Stratigraphic differentiation occurring in late Aptian–Cenomanian times, recording the onset of tectonic events differently affecting the aforementioned domains, likely related to the opening of oceanic seaways in the CEIM and the SSZ.

https://doi.org/10.1016/j.jseaes.2023.105736

GRAPHICAL ABSTRACT

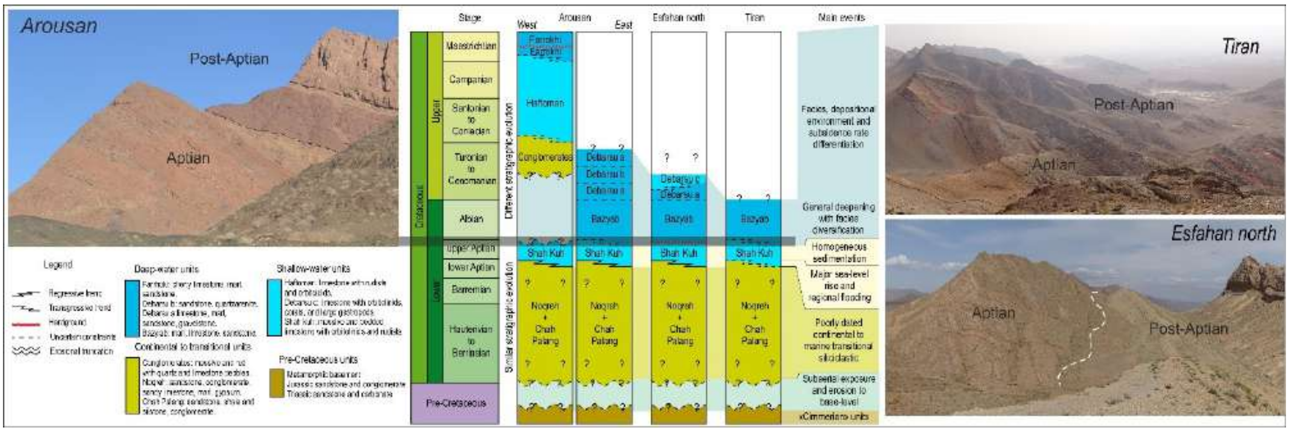

1. Introduction

The Cretaceous is a “*Greenhouse Period*” (e.g., Rothman, 2002) characterized by high sea-level conditions that favoured the development of large epicontinental seas, where transgressive marine Cretaceous sediments were deposited (Schlanger and Jenkyns, 1976; Spicer and Corfield, 1992; Jarvis et al., 2002; Fluteau et al., 2007; Hay, 2008; Hay and Floegel, 2012; Hu et al., 2012; Wagreich et al., 2014; Haq, 2014; Sames et al., 2016; Niechwedowicz et al., 2021; Yao et al., 2022). The study of Cretaceous successions, covering large, eroded areas, is critical to understand the timing and the significance of the Cretaceous transgressions and to identify local, regional, or possibly global events able to create the accommodation space required for the preservation of Cretaceous sediments. In Iran the rapid, widespread Cretaceous transgression is well documented all over different domains (Fig. 1): almost ubiquitous shallow-water carbonates non-conformably cover a low-relief surface recording the deep erosion of the Cimmerian Orogen that predates the reprise of marine sedimentation after long-lasting non-depositional and/or erosional periods (Berra et al., 2007; Wilmsen et al., 2009). The Cimmerian Orogeny produced during Late Triassic–Early Jurassic an orogenic belt recording the collision of peri-Gondwanan plates along the Eurasia – margin after the subduction of the Paleotethys ocean (Berberian and King ,1981; Alavi, 1991; Alavi et al.,1997; Boulin, 1991; Ruttner, 1993; Wilmsen et al., 2009; Zanchi et al., 2009a). Early Jurassic metamorphism and deformations, identified in several areas of NE and Central Iran (Agard et al., 2005; Rahmati-Ilkhchi et al., 2011; Zanchi et al., 2015; Sheikholeslami and Kouhpeyma, 2012; Sheikholeslami et al., 2019; Gyomlai et al., 2022), point to compressive deformations persisting also during Early and Middle Jurassic. Early Jurassic subduction of continental crust has also been recognized along the Sanandaj–Sirjan active margin in Chadegan, where eclogites provided $^{40}Ar/^{39}Ar$ ages ranging from 184.3±0.9 to 172.5±0.8 Ma (transition between Early and Middle Jurassic; Davoudian et al., 2016). After the closure of the Paleotethys and the Cimmerian events, the Iranian microplate was characterized by a post-orogenic deep erosion, predating the Early to Late Cretaceous

https://doi.org/10.1016/j.jseaes.2023.105736

transgression. At a regional scale, the Late Cretaceous evolution is characterized by the opening of seaway floored with oceanic crust (Sabzevar ophiolites in the north, Inner Zagros and Outer Zagros ophiolites in south-southwest; Shojaat et al., 2003; Moghadam et al., 2014; Sistan to the east, Jentzer et al., 2022) before the closure of the Neotethys Ocean (Agard et al., 2005). The Cretaceous successions were later affected by severe shortening due to the closure of the Mesozoic oceanic basins and to the multiphase activation of major strike-slip faults occurring during the Cenozoic up to the Quaternary (Farbod et al., 2011; Javadi et al., 2013, 2015; Tadayon et al., 2019; Zanchi et al., 2021). Despite this complex setting, it is possible to reconstruct the Cretaceous stratigraphic evolution in the different Iranian domains (Fig. 1). From the Kopeh Dagh area of the NE Iran domain, to the Sanandaj–Sirjan Zone (SSZ), the Early Cretaceous transgression led to the development of a large epicontinental sea, storing marine sediments unconformably resting on different units, represented by deformed older sedimentary successions or crystalline basement.

The Cretaceous successions of different Iranian domains have been the subject of many contributions during the last years (e.g., Wilmsen et al., 2013; 2015; 2018a; 2018b; Babaahmadi et al., 2021; Gheiasvand et al., 2021; Raisossadat et al., 2021; Sharafi et al., 2021; Yazdi-Moghadam et al., 2021), including its relationships with magmatic activity (Monsef et al., 2022). However, the state of knowledge remains incomplete and more data from different areas of the Iranian puzzle are needed. The present work is focused on outcrops belonging to three Cretaceous successions: Arusan, Esfahan north area, and Tiran (Fig. 1). The study of the Cretaceous successions and their evolution is expected to provide a contribution to the understanding of the geological evolution of the CEIM and SSZ and to provide hints on the possible controlling factors driving the timing and significance of the stratigraphic events recorded by the Cretaceous successions.

The study of the stratigraphic evolution of the transgressive Cretaceous units in different domains of the complex Iranian jigsaw is expected to highlight possible similarities and differences in the considered domains of Iran. Aim of this research is the identification of common and different patterns, as well as their interpretation in terms of extrabasinal or regional controlling factors and dating through the biostratigraphic constraints obtained from the study of the selected successions.

The selected areas (Fig. 1) are (i) Arusan (north of Khur), (ii) north-east of the city of Esfahan (iii) and in the surroundings of the village of Tiran (Fig. 2). The three zones are part of different domains in Iran. The Arusan area belongs to the Yazd Block of the CEIM, the area north of Esfahan is placed in a complex region at the transition between the CEIM and SSZ (or “complexly deformed zone” of the Sanandaj–Sirjan; Mohajjel et al., 2003), whereas the Tiran outcrops likely belong to the SSZ. The uniform approach to the study of the three areas may provide crucial information about the stratigraphic and environmental evolution, useful to identify major events differentiating the Iranian domains during the Cretaceous, and to identify common lithostratigraphic units in the studied successions.

https://doi.org/10.1016/j.jseaes.2023.105736

2. Geological setting and Cretaceous successions in Iran

Cretaceous successions in Iran have a wide distribution from the Alborz and Kopeh Dagh in the North to the Zagros belt in the south (Fig. 1). They record a regional reprise of sedimentation after the deep erosion of the Cimmerian orogeny, followed by the development of internal seaways floored with oceanic crusts, documented by the present-day complex distribution of ophiolitic belts (Moghadam et al., 2021; Pirnia et al., 2020). The extensional tectonics related to the opening of these oceanic basins is documented by rapid facies and thickness changes of the Cretaceous successions (Zanchi et al., 2015, 2021; Moghadam and Stern, 2021; Monsef et al., 2022).

The present-day Iranian plateau consists of a composite continental lithosphere made of blocks detached from Gondwana during the Palaeozoic (Stöcklin, 1974; Sengor, 1979, 1984, 1990; Dercourt et al., 2000; Angiolini et al., 2007; Fig. 1). The CEIM, including the Yazd-Tabas-Lut blocks, represents the central part of the Iranian microplate, bordered by the Alborz and Kopeh-Dagh to the north, SSZ and Zagros belt to the south-west, and the Sistan Belt and Makran to the south and to the east (e.g., Dercourt et al., 2000). On the basis of the present-day distribution of continental blocks, the CEIM was likely separated from the southern Eurasian margin by narrow oceanic basins during Cretaceous times: the Sistan Ocean to the east, the Sabzevar Ocean to the north, and the Naein–Baft Ocean to the west (Lindenberg et al., 1983; Tirrul et al., 1983; Dercourt et al., 1986; Dercourt et al., 2000; Barrier and Vrielynck, 2008a, 2008b; Moghadam et al., 2014; Gyomlai et al., 2022; Jentzer et al., 2022). The complex distribution of the ophiolites around CEIM is still a matter of debate (e.g., the interpretation of the Naein ophiolite as part of the Sabzevar Ocean displaced by the Great Kavir-Doruneh Fault System; Pirnia et al., 2020; Zanchi et al., 2021). The present-day position of the Naein ophiolite (closer to the Baft than to the Sabzevar ophiolite) is ascribed to the two-stage counterclockwise rotation of the CEIM (Mattei et al., 2015; Pirnia et al., 2020) along the Great Kavir-Doruneh Fault System and its precursors, occurring before Pliocene, when the fault system was active with a dextral sense of movement (Javadi et al., 2013; 2015; Zanchi et al., 2021). The first stage of rotation taking to an average rotation of about 35° (Mattei et al., 2015) occurred during the Early Cretaceous and may have influenced the opening of the coeval oceanic basins surrounding the CEIM (Wilmsen et al., 2021).

The various small oceanic basins around the CEIM (Fig. 1) began closing during the latest Cretaceous and Paleogene, due to the subduction of the Neotethys ocean, predating the collision of the Arabian Plate with the Eurasian margin in the late Cenozoic (e.g., Tirrul et al., 1983; Dercourt et al., 1986; Stampfli and Borel, 2002; Agard et al., 2005; Rossetti et al., 2010).

The Cretaceous succession in most of the Iranian domains (e.g., CEIM, Alborz, SSZ) unconformably covers older successions or crystalline basement made of metamorphic and igneous rocks, postdating a deep erosion that smoothed the Cimmerian topography. Postdating the Cimmerian orogeny, during Early Cretaceous a general levelling of the relief occurred: palaeo-valleys were filled with clastics and highs were

https://doi.org/10.1016/j.jseaes.2023.105736

progressively denudated. Therefore, at the beginning of the Aptian, the Iranian microplate mostly was a low-relief area facing the Neotethys, where deeply eroded older units alternate with depressions filled with continental sediments (Wilmsen et al., 2015), generally referred to as Chah Palang Formation of the Yazd Block or equivalent units (e.g., Sangestan Formation). This low-relief area was covered at a regional scale, since the Aptian, by marine Cretaceous sediments (Early Cretaceous transgression; e.g., Wilmsen et al., 2015). Some low-relief highs persisted until the Late Cretaceous, as documented by the age of the oldest sediments covering them. Upper Cretaceous sediments unconformably and non-conformably cover older units in the Neka Valley in the Alborz belt (Berra et al., 2007), the Triassic units of Nakhlak (Balini et al., 2009), the Anarak Metamorphic Complex in the CEIM and large parts of the Shotori Mountains (Wilmsen et al., 2005). This suggests a gradual onlap of the Cretaceous units above low-relief highs locally persisting after the major erosional event predating the regional transgression.

The post-Cretaceous deformations caused a strong uplift of the Cretaceous units in some area followed by a deep erosion s, or subsidence in others (where the Mesozoic units are covered by thick Cenozoic successions), preventing their continuous exposure. In detail, the Cenozoic tectonics strongly affected the Iranian blocks, further hampering the reconstruction of the original relationships among Cretaceous successions. Consequently, uncertainties persist in the reconstruction of the Cretaceous evolution of the Central Iranian domains and the significance of the Cretaceous ophiolitic belts that are preserved at the contact between different blocks (e.g., Sabzevar Ophiolites). The integration of new stratigraphic data is expected to provide constraints on the timing and mode of the reprise of sedimentation during the Cretaceous, resulting from the interaction of global, climatic and geodynamic controls.

Considering this complex tectonic and stratigraphic evolution, the stratigraphy of the three areas (Arusan, Tiran and Esfahan north) were studied by the measurement of stratigraphic logs (Fig. 2). As the three successions are characterized by a different post-depositional evolution, reflecting the complex dynamics of the Iranian blocks, stratigraphic analyses were accompanied by the reconstruction of the main geological field relationships and structural features of the three zones, which are here summarized as follows.

2.1 Arusan area

The Arusan area, belonging to the Yazd block, is located to the north of Khur along the southern border of the Great Kavir-Doruneh Fault System, about 50 km east of the town of Jandaq. Its structural setting is dominated by the pre-Pliocene dextral strike-slip Arusan Fault System (AFS), including several different strands, forming a possible precursor of the present-day active left-lateral Great Kavir-Doruneh Fault System (Zanchi et al., 2021). The AFS consists of several ENE–WSW dextral strike-slip faults which crop out a few kilometres to the south of the active left-lateral Great Kavir Fault along the slopes of the Kuh-e-Kalateh,

https://doi.org/10.1016/j.jseaes.2023.105736

uplifting and exposing the Cretaceous to Paleogene successions (Fig. 3). Transtensional and transpressional structures causing a local repetition of the Cretaceous succession occur in the area.

The Cretaceous succession is floored with a polymetamorphic basement showing an Early Jurassic imprint and by the Arusan ophiolitic mélange of unknown age (Bagheri and Stampfli, 2008; Torabi, 2009). Granitoids also occur along the AFS giving poorly constrained Late Jurassic K-Ar ages (158–147 Ma; Romanko, 1969). The Chah Palang Formation, consisting of continental sandstone and conglomerate, non-conformably covers the crystalline basement. According to recent works (Wilmsen et al., 2015), the unit was deposited between the end of the Jurassic and the beginning of the Cretaceous postdating Jurassic deformation and metamorphism (Rahmati-Ilkhchy, 2011; Zanchi et al., 2015).

2.2 Tiran Area

The Tiran area belongs to the non-metamorphic sector of the SSZ, which has been defined by several authors as the westernmost portion of the Iranian microplate, sandwiched between the Zagros orogen and the Urumieh–Doktar magmatic arc. The SSZ shows a marked Palaeozoic Gondwanan ancestry similarly to the units composing Central Iran, followed by a Meso–Cenozoic evolution related to an active margin (Berberian and King, 1981; Zanchi et al., 2009b; Hassanzadeh and Wernicke, 2016; Shakerardekani et al., 2021; Viaretti et al., 2021).

The study area is located to the NW of Esfahan along the Dareh-Bid-Tiran Thrust close to the tectonic boundary with the polymetamorphic units of the SSZ (Shakerardakani et al., 2021). West of this important structure, low and very low-grade Triassic to Lower Jurassic metapelites (possibly corresponding to the Shemshak Group) are coupled to eclogites recently dated to the Early Jurassic (Davoudian et al., 2016). The structural grain of the Tiran region is characterized by largely spaced NW–SE-striking, SW-verging thrust systems almost entirely developed within the Cretaceous succession, which is often severely folded and tectonically repeated along the main structures. Structural observations performed along the main thrusts suggest WNW–ESE to NW–SE-trending structures along the Daran and Dareh-Bid–Tiran Thrust, passing just to the north of Tiran.

Structural observations carried out at a mesoscopic scale along the main faults suggest a dip-slip kinematics with striations and growth fibres with almost pure reverse motions along both the Daran and the Dareh-Bid–Tiran Thrust (Fig. 4). Oblique dextral and left-lateral reverse movements occur along the Daran Thrust Fault with dextral motions, which seem to follow in time dip-slip thrusting. Folds measured along the Dareh-Bid – Tiran Fault north of Tiran (sites T-Th1; Fig. 4) show NW–SE sub-horizontal hinges with a cylindrical geometry, developing a marked axial plane disjunctive cleavage dipping to NE. West of Varposht (Site VP1), tight to isoclinal folds with vertical cleavage and axial planes develop in the fine-grained shaly to marly facies of the Lower Cretaceous succession. Fold geometry is given by thin limestone layers with reworked orbitolinid-

https://doi.org/10.1016/j.jseaes.2023.105736

limestones deposited within the deepest parts of the Early Cretaceous basin. We analysed the Dareh-Bid thrust close to the homonymous village and at Gonahran (Fig. 4). Fault planes dip to the NE with a medium angle and a layer of few meters with calc-mylonites occur along the thrust plane, indicating that deformation partially occurred in plastic conditions (Badertscher and Burkhard, 2000). Similar data have been obtained east of Ashin along a faulted anticline (Ash1) and along the contact between the Lower Cretaceous marly layers and very low-grade Jurassic meta-sandstones.

2.3 Kalahrood and Morgh area (Esfahan north)

At Morgh, the Cretaceous succession covers with a regional angular unconformity tilted and folded Triassic to Jurassic successions and it is extraordinarily evident in remote imagery in Goggle Earth. Despite the poor deformation of most of the Cretaceous outcrops, which are flat or gently tilted to the south, thrust-related folds locally occur along the ridge to the south of Morgh (Fig. 5)

The Kalahrood area consists of an ESE–WNW synclinorium continuously exposed along its core, for about 20 kilometres, the Cretaceous successions, unconformably resting on thick, mostly terrigenous, Triassic to Jurassic fine-grained successions at least partially deposited in a marine environment. Parasitic open to closed folds with a few hundred meters of wavelength characterize the internal structure of the synclinorium, showing characteristic w–shaped parasitic folds with both chevron and concentric hinge zones (Fig. 5). Here, about 150 measurements including bedding, cleavage, fold axial planes and hinges in the Lower Cretaceous units (Fig. 5; site Kalahrood) are consistent with the regional trends of the main folds, showing subvertical disjunctive cleavage and axial planes, as well as sub-horizontal E–SE plunging hinges. Flexural-slip along bedding has been locally observed with dip-slip striations.

3. Methods

Stratigraphic logs (Fig. 2) have been measured in the three studied areas, north of Khur (Arusan area), Esfahan north (Kalahrood and Morg), and close to Tiran (Fig. 1). Logs were selected according to the exposure conditions, absence of important tectonic overprint, continuity and accessibility. Samples have been collected along the stratigraphic logs for thin-section analysis. About 180 thin sections were analysed. The integration of field and thin section observations led to the identification of 11 facies types (Tab. 1), defined according to texture, structures and components. The thin sections are stored at the Dipartimento di Scienze della Terra "A. Desio" of the University of Milan. On carbonate microfacies, the classifications by Dunham (1962) and Embry and Klovan (1971) have been applied for textural features, and by Flügel (2004) for grain characterization. Original biostratigraphic data from planktonic and benthic foraminifera were obtained from thin-section analysis.

https://doi.org/10.1016/j.jseaes.2023.105736

4. Stratigraphy

The successions from the three studied areas are characterized by a comparable initiation and evolution, marked by a basal thin mixed carbonate-siliciclastic unit (from a few to a few tens of meters) rapidly evolving into shallow-water orbitolina-rich limestones. This succession commonly rests non-conformably on eroded metamorphic units involved in the Cimmerian orogeny or unconformably on underlying sediments. The stratigraphic evolution is characterized by the deposition of a basal carbonate unit, similar in the three studied areas, followed by a marked stratigraphic differentiation. The detailed comparison of the successions highlighted analogies and differences in the depositional, environmental and stratigraphic evolution. The stratigraphic organization of the three successions, the distribution (Tab. 1), and associations (Tab. 2) of the facies types is discussed separately and then compared.

4.1 Arusan area

The Cretaceous marine succession in the Arusan area (north of Khur; Fig. 6, 7) rests upon a Cimmerian-related metamorphic basement (Bagheri and Stampfli, 2008; Zanchi et al., 2021) or upon sandy coastal deposits. These siliciclastic deposits (e.g., Wilmsen, 2015) consist of up to 1000 m-thick conglomerates and sandstones (Chah Palang Formation) south of Khur (Wilmsen, 2015), covered by up to 500 m of mixed transitional facies (Noqreh Formation). In the study area, the Chah Palang Formation is discontinuous and fills depressions carved in the metamorphic rocks, whereas a possible equivalent of the Noqreh Formation is represented by a few meters of coastal sandstone with carbonate cements. Above the low-relief area represented by eroded basement rocks, the presence of a non-conformity (above basement rocks) is documented by a thin (up to 1-2 m) layer of conglomerates with calcareous cement characterized by abundant well-rounded quartz pebbles (CSS; Fig. 6A and B; 8A), denoting a high textural and mineralogical maturity. The deposition of the Cretaceous successions starts with these quartz-rich fine-grained conglomerate and sandstone with carbonate cements (CSS), making transition to orbitolinid- and rudist-bearing mixed carbonate-siliciclastic facies (HYB; Fig. 6D). The rapid transition to marine conditions is documented by carbonate facies belonging to the Shah Kuh Formation (Wilmsen et al., 2013; 2015), characterized by the abundance of orbitolinids and small rudists also in life position (RLM; Fig. 6E) from the base of the Cretaceous succession. The thickness of the Shah Kuh Formation is reduced to the west (about 35 m), whereas it ranges between 100 and 120 m toward the west.

Above the Shak Kuh Formation, the stratigraphic evolution of the eastern and western part of the study area differs. In the western sector, immediately above the Shah Kuh Formation, a sharp fine-grained silicilastic input, represented by about 4 m of bedded limestone with quartz grains and fenestral texture (OBL) is recorded: the siliciclastic input is also documented by the abundance of orbitolinids incorporating quartz micrograins in the shells (OBL; Fig. 8H), extremely abundant in this stratigraphic interval. This interval is

https://doi.org/10.1016/j.jseaes.2023.105736

rapidly covered by about 50 meters of massive red conglomerates with alignment of abundant quartz (up to 5 cm in size) and limestone pebbles (Fig. 6F; CGL). Conglomerates are massive to faintly bedded and reflect different events of deposition, possibly represented by two major cycles. The colour is red.

Moving eastward, of Arusan, the stratigraphic evolution is different: conglomerates are absent, substituted by sandstone rich in quartz grains (QTZ; Fig. 8D), developed within a marly/silty succession (MRL) rich in echinoid, resting above massive limestone of the Shah Kuh Formation.

Above the conglomerates, a renewed carbonate deposition is recorded across the studied area, with a rapid transition, marked by a few meters of bedded, fine-grained limestone, to another massive carbonate unit, consisting of bioclastic limestone rich in rudists, ostreids and abundant orbitoidids (ODL; Fig. 9E), thus documenting its Late Cretaceous age. This carbonate unit is referred to as Haftoman Formation (Wilmsen et al., 2015, 2018a) and represents an extended carbonate platform. The Haftoman Formation, ranging in thickness from about 50 m to 150 m, is dominated by bioclastic packstones rich in rudists (RLM; Fig.), reworked and in life position. Well-rounded quartz pebbles from a few millimetres to about 1 cm are locally present.

The massive Haftoman Formation is covered by about 20 to 30 m of alternating limestone (RLM and ODL; mostly bioclastic packstone) and marls that are interpreted as the topmost part of the unit. The decrease in carbonate production and the abundance of marls (60 to 65 m), locally bioturbated, with disperse echinoids (MRL), marks the transition to the Farrokhi Formation (Fig. 7A). The reprise of carbonate production, postdating the deposition of marls, is sharp (Fig. 7C) and represented by bedded, bioturbated limestones, locally with quartz grains, with rare chert nodules (CHL; Fig. 7E). The microfacies typically consists of wackestone to packstone with abundant planktonic foraminifera, radiolarians and calcispheres (CHL; Fig. 8G; 9H). The upper boundary of this unit is represented by a hardground with glauconitic crusts, poorly preserved ammonites, belemnites, gastropods, echinoids, and bivalves (HGL; Fig. 7F, G; 9F and G). Above this hardground, the succession is dominated by a marly unit containing rare calcareous beds and characterized by abundant bioturbations (CHL; *Thalassinoides* and *Zoophycus*). The youngest part of the succession (Fig. 7A, I) is represented by bedded cherty limestone (CHL; Fig. 9H), with a thickness of more than 200m.

Stratigraphic evolution

The transition from a deeply eroded basement to shallow-water marine conditions is represented by the deposition of quartz-rich fine-grained conglomerate and sandstone with carbonate cements (CSS) and a thin hybrid limestone unit (HYB) at the base. This unit rapidly evolves to a massive limestone unit with rudists and orbitolinids (RLM and OBL) that can be traced across the studied area, denoting a rapid marine transgression and environmental change. This carbonate unit, the Shah Kuh Formation, documents the development of an

https://doi.org/10.1016/j.jseaes.2023.105736

epeiric sea in tropical climate, characterised by uniform facies distribution. The tabular geometry of the unit describes a stable geodynamic setting, with a shallow-water sea expanding across the studied area.

The presence of conglomerates (CGL) above the Shah Kuh Formation, which is characterized in its upper part by bedded bioclastic limestone (OBL) alternating with marly interlayers (MRL), can be continuously traced in the studied area, documenting the erosion of carbonate facies and the availability of quartz deriving from basement highs. This interval is characterized by faint laminations and alignment of clasts and red colour, suggesting the transition to continental conditions in the western part of the studied area. Marine conditions persisted to the east, where the siliciclastic input is still recognizable, but it is represented by a sandstone layer embedded within a marine marly/silty succession characterized by abundant echinoids and bioturbations. The presence of conglomerate with carbonate and quartz clasts (CGL) documents the erosion of nearby carbonate highs up to the underlying basement, previously not exposed during the deposition of the Shah Kuh Formation. The abundance of quartz indicates that erosion probably reworked basal conglomerates rather than the underlying basement, suggesting a limited depth of the erosional surface.

The siliciclastic facies are rapidly covered, in the west, by a carbonate unit, which marks the return to shallow marine conditions, with abundant rudists (RLM, ODL). This unit (Haftoman Formation) is covered by alternating bedded limestone and marls, recording a drowning of the carbonate platform followed by the deposition of marls, marking the transition to the Farrokhi Formation, consisting of intervals dominated by marls (MRL) alternating with bedded cherty limestone (CHL; Fig. 7A, I). These facies mark a complete change in the depositional conditions: since the lower marly unit (M1), the succession is characterized by deep-water fossil associations (foraminifera, ammonites, belemnites, radiolarians). The reprise of carbonate sedimentation (CHL) is represented by bedded cherty limestone with bioturbations. This deep-water limestone unit is characterized at its top by a hardground with glauconite and characterised by intense bioturbation and concentration of ammonites, belemnites and echinoids (HGL). Open marine conditions persist after the development of this hardground, as documented by the deposition of marls with rare cherty limestone beds (MRL, CHL) that rapidly pass to of a second unit of well-bedded cherty limestone (CHL).

The overall evolution of the succession of Arusan records a rapid and widespread marine transgression on a previously continental area, with the homogeneous deposition of rudists and orbitolinids bearing limestone (Shah Kuh Formation). A return to continental conditions is observed westward, with deposition of conglomerates, whereas to the east marine conditions persist, with deposition of marls and siltstones, but with a quartzarenites layer probably recording the same regression responsible for the deposition of conglomerates toward the east. Differentiation of depositional conditions at a local scale suggests tectonic control on sedimentation. After a return to carbonate platform conditions (Haftoman Formation) a drowning is documented by the deposition of marls and cherty limestone, reflecting a rapid subsidence, with the deposition of the different facies of the Farrokhi Formation. The presence of poorly preserved dinosaur

https://doi.org/10.1016/j.jseaes.2023.105736

footprints (Wilmsen et al., 2022) discovered south of the study area suggests a regression at the top of a calcareous unit (Middle Limestone Member of the Farrokhi Formation). The intertidal-supratidal conditions suggested by the possible dinosaur footprints are not documented in the study area.

4.2 Tiran area

The studied outcrops (Fig. 10) are located close to the village of Tiran, in an area involved in a Cenozoic fold-and-thrust belt. Despite the occurrence of intense deformations, a continuous log cropping out east of the village was measured. The succession belongs to the “complexly deformed zone” of the Sanandaj–Sirjan zone (Mohajjel et al., 2003), where Triassic and Jurassic siliciclastic units (quartz-rich, reddish siltstone and sandstone) are sharply unconformably covered by transgressive, thick marine Cretaceous carbonate and marly units. The recrystallization, folding and intense cleavage suggest a significant burial and heating of the succession, recording erosional and/or exhumation events postdating the deformation. The Cretaceous succession unconformably rests upon poorly constrained Triassic or possibly Jurassic sandstone and siltstone, documenting an important stratigraphic gap. The base of the Cretaceous succession is characterized by a few meters of quartzarenite, conglomeratic sandstone and siltstone (CSS, about 20 m). These facies are rapidly covered, with a sharp contact (Fig. 10B), by hybrid carbonates containing quartz grains (HYB). The decrease of siliciclastic grains occurs rapidly, and about 5 m above the contact with the underlying sandstone, extrabasinal clasts disappear. The basal carbonate facies mostly consist of poorly bedded dolomitized packstone and wackestone with orbitolinids (OBL, Fig. 8E). The onset of carbonate production documents a rapid marine transgression, producing up to about 270 m of a monotonous succession of limestone, frequently irregularly dolomitized (dolomitized patches are marked by a brown colour in alteration; Fig. 10D), with bivalves, rudists and orbitolinids (RLM and OBL); bioturbations are locally present. Above this massive limestone, it is possible to observe the transition to alternating marls and siltstones (MRL) and limestone with silicified fossils (mostly bivalves, e.g., cf. *Rastellum carinatum* (Lamarck), Fig. 10E) and chert nodules (CHL, Fig. 10G). Lenticular carbonate lenses (from 1 to 5 m thick on average) interfinger with the marly, marly limestone and siltstone facies (MRL, Fig. 10H). Carbonate lenses consist of packstone/wakestone; among skeletal grains crinoids are common, orbitolinids are often abundant (OBL). Reworked rudists are rare; ostreids are locally present (RLM). The measured thickness of this unit reaches more than 200 m.

Stratigraphic evolution of the Tiran succession

In the Tiran Area, after a long period of erosion of the Triassic and Jurassic units, the base of the Cretaceous succession documents the creation of accommodation space with the reprise of sedimentation, with the deposition of a basal siliciclastic unit characterized by high mineralogical maturity, being characterized by abundant quartz grains and pebbles (CSS and HYB). The transition to bioclastic limestones (OBL and RLM)

https://doi.org/10.1016/j.jseaes.2023.105736

reflects a rapid marine transgression, with the transition to shallow-marine depositional environments, documented by the onset of carbonate deposition and a rapid decrease in the siliciclastic content. This evolution confirms that carbonate sedimentation occurred on a flattened, deeply eroded surface: after the basal transgression, no significant sources of siliciclastic sediments is preserved. After a period of persisting shallow-water depositional conditions (recorded by the massive carbonate unit), a rapid deepening is documented by the alternating marls and siltstone (MRL) and cherty limestone (CHL), with resedimented skeletal grains (ODL). The lenticular geometry of the limestone beds is interpreted as the evidence of carbonate resedimentation from shallower nearby areas.

The age of this succession is poorly constrained, but the presence of orbitolinids documents in all the carbonate facies (from the lowermost to the uppermost preserved horizons) an Aptian to, at most, Cenomanian age (Velić, 2007; Chiocchini et al., 2008). The presence of reworked, silicified ostreids (*Rastellum carinatum;* Fig. 10G) provides environmental indications, as it is considered to not tolerate salinity variations (Carter, 1968; Jablonsky and Lutz, 1980; Freneix and Viaud, 1986).

4.3 Kalahrood and Morgh area (Esfahan north)

North of Esfahan (Morgh, Fig. 11; and Kalahrood, Fig. 12), the Cretaceous succession rests with an angular unconformity upon deformed sedimentary successions. Consequently, the Cretaceous succession unconformably covers different stratigraphic units: in the studied area, the Cretaceous units cover marine mixed sediments of Triassic and Jurassic age at Morgh and quartzarenites and conglomerates with quartz pebbles possibly of Triassic and Jurassic age, at Kalahrood. Above a deeply eroded and levelled, flat surface, the Triassic to Jurassic deformed sediments are covered by red sandstone and fine-grained conglomerate (CSS) that are characterized by intercalations of bioclastic sandy limestone beds (HYB, Fig. 11B, C, D), marking the onset of the Early Cretaceous sedimentation. This unit can be traced across the studied area with the same thickness and facies association, independently from the nature of the underlying bedrock (Fig. 11A, 10B). The carbonate content rapidly increases in the upper part of the basal unit, leading to the development of a massive carbonate unit characterised by the abundance of rudists. Facies are mostly represented by skeletal packstones rich in orbitolinids and bivalves, mostly ostreids and rudists (RLM and OBL; Fig. 12D; 8F). These facies can be traced across the studied area, recording homogeneous depositional conditions, followed by a relative differentiation. Carbonate facies persist to the north (Kalahrood), whereas in the south (Morgh) a rapid transgression is documented by a glauconitic hardground (HGL, Fig. 9A; 12E) at the top of the carbonates and by the deposition of a marly unit containing ammonites and planktonic foraminifera (CHL and MRL, Fig. 9C and D).

https://doi.org/10.1016/j.jseaes.2023.105736

A return to shallow-water carbonate deposition is recorded by a prograding unit mostly made of skeletal packstones rich in rudists, gastropods (including nerineids), corals, possibly stromatoporoids, large benthic foraminifera (abundant orbitolinids), and planktonic foraminifera (RLM, OBE, Fig. 9B; Fig. 12 C, F, G, H) that represents the youngest unit cropping out in the studied area.

Stratigraphic evolution

The Cretaceous succession rests, along a regional angular unconformity, upon a flat erosional surface developed at the top of Triassic and Jurassic deformed sediments mostly consisting of quartz-rich sandstone, conglomerates and limestone. The Cretaceous succession documents a very rapid transgression with the deposition of a few meters of mixed siliciclastic and carbonate facies (CSS and HYB), passing to a massive to bedded carbonate unit rich in orbitolinids and bivalves (mostly ostreids and rudists; RLM and OBL) showing a rapidly decreasing siliciclastic content. In the lower part of the carbonate unit, a continuous interval, up to 5-7 m thick, of marly limestone is present. This evolution is observed both at Morgh and Kalahrood, but the overlying evolution is partly different and the succession at Morgh is best preserved.

Whereas at Morgh the massive bioclastic carbonate evolves to bedded and darker bioclastic limestones (up to the top of the studied succession), at Kalahrood, the top of the bioclastic carbonate unit is characterized by a hardground (HGL). This hardground marks the demise of the carbonate production and a rapid deepening, with transition first to hybrid limestone (with quartz grains) and later to marl and siltstone (MRL) with a gradual increase in the limestone content, and up to limestone with incipient chert nodules containing poorly-preserved ammonites and planktonic foraminifera (CHL). The overlying thick marly interval (MRL) still records low-energy subtidal water conditions. The top of this unit records a return to carbonate sedimentation, with the progradation of a low-angle downlapping of massive limestone rich in corals, nerineid gastropods and orbitolinds (OBE) that marks the onset of a carbonate platform and the return to shallower bathymetric conditions, with the reprise of shallow-water, high-energy carbonate sedimentation.

5. Paleontological associations and age constraints

The three studied successions cover stratigraphic intervals characterized by a coeval base but extending differently in age at the top: the Arusan succession preserves the lowermost faunal associations, followed by the Kalahrood and Morgh (Esfahan north), and Tiran. The distribution of the foraminifera in the stratigraphic logs defines different associations (Fig. 13) that provide constraints on the age of the studied succession. The abundance of foraminifera changes in the three sections that are here described separately.

https://doi.org/10.1016/j.jseaes.2023.105736

5.1. Microfossils from the Arusan area

The stratigraphic sections from the Arusan area are characterized by the presence of two well-diversified foraminifera assemblages (Fig. 13, 14). The first assemblage (assemblage A) is composed by orbitolinids such as *Praeorbitolina cormiy* Schroeder (Fig. 14A*), Palaeodictyoconus* cf. *actinostoma* Arnaud-Vanneau and Schroeder (Fig. 14B), orbitolinid indet. (Fig. 14C), *Praeorbitolina* aff. *claveli* Schlagintweit et al. (Fig. 14D), *Dictyoconus pachymarginalis* Schroeder (Fig. 14E), which are among the main constituents at stratigraphic logs K0 (lower part), K1, and K3 (Fig. 2). The taxa *Quinqueloculina* sp., *Nezzazata* sp., *Nezzazata isabellae* Arnaud-Vanneau and Sliter (Fig. 14F), *Akcaya minuta* (Hofker) (Fig. 14G), *Cuneolina* sp., *Cuneolina* cf. *hensoni* Dalbiez (Fig. 14H) complete the A assemblage. Furthermore, calcareous algae and bacinellid textures are occasionally present. Planktonic foraminifera *Globigerinelloides* sp., *Whiteinella* sp., *Whiteinella baltica, Whiteinella brittonensis*, *Muricohedbergella delrioensis*, *Praeglobotruncana stephani* and calcispheres mainly occur in the easternmost sector (Log K4) of the Arusan area and define "assemblage B". Samples from K0 (upper part), K2, and K9 do not contain orbitolinids and the other taxa occurring in assemblage A, but they yield abundant *Siderolites calcitrapoides* Lamarck (Fig. 14I), *Orbitoides* sp., and *Orbitoides media* (D'Archiac) (Fig. 14J, K) that are often associated with the red algae *Paraphyllum amphiroaeformae* (Rothpletz) (Fig. 14L). The association of these taxa allows the identification of assemblage C. Gastropods, ostracods, rudists, bryozoans, echinoderms, and brachiopods are abundant in both assemblages A and C.

5.2. Microfossils from the Esfahan north area

As in the Arusan area, two main assemblages can be distinguished in the Esfahan north area (Fig. 15). Orbitolinids dominate the lower part of the studied logs and *Iraqia* cf. *simplex* (Fig. 15A) and several orbitolinid (Fig. 15B) have been observed. Other benthic foraminifera are *Balkhania balkhanica* Mamontova (Fig. 15C), *Torremiroella hispanica* Brun and Canérot (Fig. 15D), that together with the calcareous algae *Permocalculus* sp., *Neomeris* sp. *Bakalovaella elitzae* (Bakalova) (Fig. 15E) and bryozoans allow identification of the A1 assemblage. In the Esfahan north area, planktonic foraminifera (i.e., *Whiteinella* sp.; *Whiteinella brittonensis* (Loeblich and Tappan), Fig. 15F, G; *Whiteinella baltica* Douglas and Rankin, Fig. 15H, I; *Helvetoglobotruncana praehelvetica* (Trujillo), Fig. 15J; *Muricohedbergella* sp., *Muricohedbergella delrioensis* (Carsey), Fig. 15K, L; *Muricohedbergella planispira* (Tappan), Fig. 15M, N) characterize the B1 assemblage that has been observed in the upper part of the considered logs (Fig. 2).

5.3. Microfossils from the Tiran area

A single assemblage characterizes the only considered stratigraphic section of the Tiran area. Abundant specimens of the family Orbitolinidae, smaller benthic foraminifera, bryozoans, echinoid spines, and

https://doi.org/10.1016/j.jseaes.2023.105736

gastropods occur. Although no specific biomarkers have been identified, the assemblage of the Tiran area is comparable to the A and A1 assemblages observed in the Arusan and Esfahan north areas, respectively.

6. Discussion

6.1 Fossil distribution and age

In the Arusan area, the benthic foraminiferal assemblage A (Fig. 2, 13) characterizes the basal Cretaceous carbonate unit (Shah Kuh Formation and equivalent units) and is characterized by abundant orbitolinids, leading to the identification of a well-defined, restricted stratigraphic distribution. According to the data from the literature, *Praeorbitolina cormyi* is reported to occur in the upper part of the lower Aptian (late Bedoulian *sensu* Breistroffer, 1947) of the Arabian Plate (Masse, 2003; Schroeder et al., 2010; Schlagintweit et al., 2013a; Schlagintweit and Rashidi, 2022). *Paleodictyoconus actinostoma* has been reported from the lower Aptian of Central Iran (Arnaud-Vanneau and Schroeder, 1976; Wilmsen et al., 2020; Schlagintweit and Rashidi, 2022) and the upper part of the lower Aptian (southern France; Schlagintweit et al., 2013a). *Iraqia simplex* shows a similar stratigraphic distribution (late Bedoulian *Auct.* of the European and Arabo-African Tethyan margins; Masse, 2003); *Praeorbitolina claveli* was described from the lower-middle Aptian (upper Bedoulian–lower Gargasian *sensu* Breistroffer, 1947) of Central Iran (Schlagintweit et al., 2013a). *Dictyoconus*? *pachymarginalis* is frequently mentioned to occur in the lower-middle Aptian interval of the northern and southern Tethyan margins, as in the Alborz (Schroeder, 1965), in the Central Apennines (Mancinelli and Chiocchini, 2006), and in Central Iran (Schlagintweit et al. 2013a, 2013b). Therefore, the stratigraphic distributions of the marker species composing assemblage A allow inferring an early Aptian (late Bedoulian *Auct.*) age for logs K0 lower part, K1, and K3 from the Arusan area (Fig. 2). The benthic foraminiferal assemblage observed at the base of the Shah Kuh Formation in the Esfahan north area (assemblage A1) yield *Iraqia simplex*, *Balkhania balkhanica*, and *Torremiroella hispanica*, thus suggesting an early Aptian age. The species *B. balkhanica*, and *T. hispanica* are commonly recorded from Barremian to lower Aptian (Late Bedoulian–Gargasian *Auct.*) successions and characterize the Carpatho-Cimmerian bioprovince (Eurasian margin of the Neo-Tethys, Abad et al., 2013; Schlagintweit et al., 2013b; Wilmsen et al., 2020). In summary, the biostratigraphic data suggest an early Aptian age for the regional transgressive phase observed in the Arusan and Esfahan north areas.

Planktonic foraminifera are observed in the overlying samples of both the two areas (e.g., M50, M60, M74bis: see Fig. 15), recording a low diversity assemblage mainly composed by long-ranging species (assemblages B and B1; Fig. 13). However, the occurrence of *Whiteinella brittonensis*, *W. baltica*, *Muricohedbergella planispira*, *M. delrioensis*, and *Helvetoglobotruncana praehelvetica* poorly constrains the sampled units to a Cenomanian–Turonian time interval according to the known stratigraphic distribution of these species (e.g., Premoli Silva and Sliter, 1994; Robaszynski and Caron, 1995; Huber et al., 2016; Petrizzo et al., 2020; Gale et

https://doi.org/10.1016/j.jseaes.2023.105736

al., 2020) and in the absence of diagnostic zonal marker species. The occurrence of orbitolinids at the base and in the prograding bioclastic carbonates in the upper part of log Morgh (Esfahan north area) indicates an early-middle Cenomanian age for the studied interval.

The association of taxa *Siderolites calcitrapoides, Orbitoides media, Paraphyllum amphiroaeformae* that occur in logs K0 (upper part), K2, and K9 characterizes the assemblage C in the Arusan area, documenting a Maastrichtian age (Baumfalk, 1986; Baumfalk and Van Hinte 1985; Özcan et al., 2021), younger than the Santonian-Campanian age documented by Wilmsen et al. (2018a) for the Haftoman Formation. Assemblage C documents that in the study area the Haftoman Formation extended to the Maastrichtian: here, carbonate platform conditions persisted, while in the south, at the same time, the Farrokhi Formation was deposited in basinal conditions (Wilmsen et al., 2018a).

6.2 Stratigraphic evolution

The Cretaceous Period is characterized by rapid depositional changes in all the different domains that are presently arranged in the Iranian tectonic puzzle. Despite the post-depositional tectonics related to different geodynamic events (including the opening and closure of seaways among these blocks during the Cretaceous, the Zagros orogeny and the Cenozoic wrench tectonics), it is possible to reconstruct some major events characterized by both common and different stratigraphic evolutions at different localities (Fig. 16), recorded by changes in the facies associations (Tab. 2).

The most striking event that characterizes the Lower Cretaceous succession in the studied areas, in terms of distribution and lateral traceability, is the rapid spread of mixed carbonate-siliciclastic deposits followed by rapid and coeval deposition of carbonate facies all over a wide area of the Iranian territory. The continuous distribution of the Cretaceous sediments on the different blocks building the present-day Iran indicates that a wide area was rapidly inundated by the deposition of mixed siliciclastic-carbonate coastal sediments rapidly and invariably covered by shallow-water carbonates. The latter are characterized by abundance of orbitolinids and rudists. The Lower Cretaceous units are thus generally known as "Orbitolina Limestone", obtaining different names in different domains (Tirgan Formation in the Kopeh Dagh, Tizkuh Formation in the Alborz, Daryan Formation in SW Iran, Taft Formation and Shah Kuh Formation in Central Iran and south of Esfahan, or, generically, "thick bedded limestone to argillaceous limestone" in the Tiran area).

The age of the basal facies of the Cretaceous succession, constrained in age by assemblage A, is mostly Aptian, documenting that most of the central portion of Iran was covered by a shallow epicontinental sea where carbonates variably mixed with siliciclastic sediments were deposited (Fig. 16). The Cretaceous transgression occurred on a flat erosional surface, as documented by the planar geometry and lateral continuity of the Cretaceous units. This evidence indicates that, after the Cimmerian Orogeny and its late deformations (persisting during the Jurassic, as documented by the pre-Cretaceous deformation of Jurassic successions), the entire Iranian area was eroded up to the erosional base level before the rapid and widespread Lower

https://doi.org/10.1016/j.jseaes.2023.105736

Cretaceous transgression. Biostratigraphic constraints indicate an early Aptian age for the major transgression event, which is interpreted to have determined the unconformable deposition of the "Orbitolina Limestone" and of the equivalent marine carbonate units above the Cimmerian terranes (e.g., Wilmsen et al., 2010; 2013). The deposition of limestone containing rudists and orbitolinids and characterized by a decreasing (from the base to the top) amount of mineralogically mature siliciclastic facies is observed in all the studied area, belonging to different tectonic domains: the Yazd Block, the non-metamorphic sector of the Sanandaj–Sirjan Zone, and western CEIM. Similar units are observed also in the Alborz, whereas in the Kopeh Dagh the Cretaceous succession conformably rests upon Jurassic units and consists of alternating carbonate and fine-grained siliciclastics (Taheri et al., 2009; Robert et al., 2014). The presence of several hiatuses within the Cretaceous to Paleocene successions in the NE part of the belt is interpreted as the evidence of local uplifts, suggesting a Late Cretaceous-Paleocene tectonic reactivation of the belt (Wilmsen et al., 2013; 2015; Robert et al., 2014). In the late Turonian, the area has been subject to a major tectonic event that caused a tilting of north-dipping fault blocks with widespread erosion and karstification on the crests (Wilmsen et al. 2015), documenting the erosion of up to 2000 m of Cretaceous sediments. Only rarely, possibly above persisting highs, the age of the Cretaceous transgression is slightly younger. In the northern Alborz, the transgression is Late Cretaceous on Cimmerian highs (Santonian, Neka Valley; Berra et al., 2007); similarly, at Nakhlak, the transgressive carbonate facies that directly cover a deformed Triassic succession (Balini et al., 2009; Zanchi et al., 2009b) are Late Cretaceous in age (see also Vaziri et al., 2005; 2012). The Cretaceous succession resting above the Anarak metamorphic units (Zanchi et al., 2015) shows a roughly constant thickness, suggesting that also here deposition occurred on a low-relief area due to a rapid marine transgression. The continuity and homogeneous facies of the Aptian strata across different Iranian domains indicate that deposition occurred on a low relief area produced by the erosion of a tectonically stable continental area, except for small highs where deposition starts during the Late Cretaceous. These highs are interpreted as low-relief islands in an epeiric sea, where shallow-water carbonate sediments were deposited. The rapid Cretaceous marine transgression on the post-Cimmerian peneplain occurred after a long period of subaerial erosion, as documented by the high textural and mineralogical maturity of the siliciclastic sediments at the base of the Cretaceous succession, typically represented by well-rounded quartz grains in conglomerate and quartzarenite, independently from the composition of the underlying successions. The presence of calcite cements and skeletal grains (typically orbitolinds) from the base of the Cretaceous succession suggests a very rapid transition from continental to marine sedimentation.

This common and coeval evolution in distant stratigraphic successions documents the rapid marine transgression that reflects the well-known (Sloss, 1963) and abrupt flooding of continental areas observed during the late Early Cretaceous. This event is recorded in the CEIM by the deposition of Aptian carbonates on continental to coastal units (Chah Palang and Noqreh formations) of variable thickness (from a few to

https://doi.org/10.1016/j.jseaes.2023.105736

hundreds of meters), folded sedimentary units involved in the Cimmerian Orogeny, and metamorphic basement.

The age of the transgression and geometry of the sedimentary units indicate that, during the Aptian, Iran was a lowland facing the Neotethys to the south. The rapid transgression (Fig. 16) can be interpreted as the result of a major sea-level rise that, considering its wide distribution, could be more probably related to an eustatic event rather than to local subsidence. The biostratigraphic constraints indicate an early Aptian age for this rapid transgression; a higher precision is not possible with the available biostratigraphic data.

The timing of the Cretaceous transgression in Iran can be compared with global sea-level curves. The beginning of a major transgression in early Aptian is well documented on the passive margin of the Arabian plate facing the Neotethys ocean (van Buchem et al., 2010), that had a passive margin during the Early Cretaceous, recording a sea-level rise more important than that recorded by the Barremian succession: in the Arabian plate the recovery of shallow-marine deposits occurred in early Aptian (van Buchem et al., 2010). During early Aptian, the existence of a sea-level rise was also previously documented from the study of the Cretaceous succession of the Arabian plate by other authors (e.g., Sharland et al., 2001; Davies et al., 2002). This eustatic sea-level rise turned out to be coeval with the initiation of the deposition of Cretaceous marine sediments in the different domains of Iran. The rise of the sea level was sufficiently high to trigger the development of a carbonate unit dominated by large bivalves (mostly ostreids and rudists) and large benthic foraminifera (orbitolinids). The roughly constant thickness of the unit indicates a homogeneous creation of accommodation space, still suggesting a major role of an eustatic sea-level rise (of the order of several tens of meters) on a slowly subsiding area without evidence of significant tectonic activity. Origin and controlling factor of this important sea-level rise still requires further investigations, during a greenhouse period, when ice caps were likely absent. Nevertheless, a significant role of glacio-eustatic sea-level changes is suggested by Frau et al. (2020), who recognize during late Barremian a major exposure event in the Mediterranean area followed by a sea-level rise in late early Aptian, coeval with the observed major transgressive event in Iran.

The difference between the homogeneous conditions documented by the similar Aptian facies and the high differentiation (in terms of facies and thickness) of the overlying units can be ascribed to the identification of structural domains characterized by different subsidence rates, possibly reflecting the beginning tectonic disruption of the large Aptian epeiric carbonate platform. Evidence of tectonic activity is documented by erosion and deposition of sandstone and conglomerates with carbonate and quartz pebbles around Arusan, in the Esfahan north area by the development of a hardground on top of the shallow-water orbitolina and rudist limestone (followed at Morgh by a Cenomanian carbonate platform), and, at Tiran, by the transition to deep-water facies that indicates a rapid subsidence with creation of accommodation space.

A major angular unconformity, confirming this geodynamic change, was also well documented by Wilmsen et al. (2015; 2018b), who document a major erosional event predating the deposition of the Haftoman

https://doi.org/10.1016/j.jseaes.2023.105736

Formation (Coniacian in age at the base), that unconformably rests on older (Barremian to Turonian) units in the Khur area. The stratigraphic evolution is different south of Esfahan, where most of the upper Albian to middle Cenomanian succession is missing or reworked into upper Cenomanian glauconitic facies (Hairapetian et al., 2018). The succession at Morgh strongly resembles that described by Wilmsen et al. (2020) south of Chupanan, east of the Anarak metamorphic complex.

This rapid Early Cretaceous transgression is consistent with: (i) the rapid and laterally continuous development of epeiric carbonate platforms in Iran during the Early Cretaceous; (ii) a green-house period dominated by persisting high sea-level conditions. In fact, during the Cretaceous the sea level was about 100 m higher than in the Jurassic, according to all the available sea-level curves (e.g., Miller et al. 2005; Haq et al., 2014), and the increase of the flooded continental areas is recorded worldwide (Sloss, 1963). Despite the Aptian transgression starts with very similar successions in the described different domains, the different stratigraphic evolution from the Albian reflects major local tectonic events documented by rapid thickness changes and a general deepening of the successions.

6.3 Regional implications

The geodynamic significance of the stratigraphic evolution reconstructed from the three studied areas can be discussed in the frame of the Cretaceous evolution of Central Iran. During Late Cretaceous is a major tectonic re-organizations of the Iranian domains occurred. Ophiolitic belts, mostly interpreted as remnant of back-arc basins along the western border of the CEIM document the existence of oceanic seaways, whose opening is ascribed to the subduction of the Neotethys ocean under the SSZ (Esfahan–Hamadan Trough, Naein-Baft Rift, Sabzevar, producing the "Inner belt ophiolites" of Stöcklin, 1981; Ghasemi and Talbot, 2006; or to the Zagros internal belt of Moghadam et al., 2014). The origin of these oceanic basins is still debated (e.g., Barrier and Vrielynck, 2008; Omrani et al., 2013; Barrier et al., 2018; Pirnia et al., 2020; Jentzer et al., 2022). The differentiation of the three areas after a common Aptian stratigraphic evolution (Fig. 16), is recorded by changes in the subsidence rates, that reflects a new geodynamic scenario characterized by the existence of different crustal blocks separated by basins floored with oceanic crust. According to the proposed paleogeographic reconstruction (Hairapetian et al., 2018), the succession at Arusan belonged to the Yazd block during the Cretaceous and was separated by the Esfahan-Hamadan Trough, Naein-Baft Rift (or Ocean) and Sabzezvar Ocean from the Tiran succession, which was part of the Sanandaj–Sirjan block. The paleogeographic position of the Esfahan north successions is still debated, as it is located along the poorly defined boundary between the Urumieh-Dokhtar arc and the SSZ. According to Hairapetan et al. (2018), this area might be separated from Central Iran by the Sabzevar and Naein-Baft Oceans, but alternatively it might also be part of NW Iran.

https://doi.org/10.1016/j.jseaes.2023.105736

Before this differentiation the similar evolution, recorded by the comparable (for timing, facies and thickness) Aptian shallow-water transgressive marine carbonates, suggests a possible lateral continuity of the three successions. The similar sedimentation and the coeval transition from emerged land to marine epeiric carbonate deposits indicate that the geodynamic differentiation of CEIM and SSZ occurred after the Aptian transgression and likely began towards the end of the deposition of the Shah-Kuh/Taft Formation, whose demise is therefore considered as the effect of changing subsidence conditions. The increasing subsidence may be reasonably related to a general increase in the extension rates, which are consistent with the opening of the oceanic seaways separating the main crustal blocks of Iran (e.g., Esfahan-Hamadan Trough, the Naein-Baft Rift, Sabzevar). This scenario is compatible with the age of the Sabzevar Cretaceous back-arc basin, as suggested by biostratigraphic data from the Sabzevar ophiolites, associated with Upper Cretaceous basinal limestones (Shojaat et al., 2003).

Finally, the stratigraphic evolution of the studied successions suggests that the initiation of the extension leading to the opening of oceanic basins within the CEIM occurred close to the Aptian–Albian boundary. The dating of this extension, predated by a major eustatic sea-level rise in early Aptian, provides important constraints on the timing of the post-Cimmerian crustal fragmentation of Iran , taking to a new geodynamic cycle reshaping the entire microplate.

7. Conclusions

The deposition of the Cretaceous succession in Central Iran postdates a major, complex tectonic event, responsible for the docking of the Perigondwanan terranes producing the Cimmerian orogenic phases, starting at the end of the Triassic and lasting for most of the Jurassic. Facies distribution indicates that before the deposition of the Cretaceous units, deep erosion produced a flat topographic surface: above this surface, continental sediments rapidly evolve to transgressive Aptian marine carbonates, across most of the present-day Iran. After this interval of homogeneous sedimentation, a rapid stratigraphic differentiation is documented by major facies and thickness changes. This evolution, that can be observed in different parts of the Iranian geological jigsaw, has been studied in detail in three selected areas: Tiran, Arusan and Esfahan north (Kalahrood and Morgh logs).

The biostratigraphic constraints document a rapid transgression of orbitolinid- and rudist-bearing limestones at a regional scale. This transgression occurred mostly in the early Aptian, being slightly younger in some places, likely representing low relief (islands) in the Iranian, Early Cretaceous epicontinental sea. The geologically synchronous onset of the Aptian sedimentation in Iran is considered to reflect an eustatic sea level rise, able to explain the observed stratigraphic evolution. The observed Aptian transgression fits with one of the major sea-level rises recorded in the Cretaceous and is surely the most important one recorded in Iran.

https://doi.org/10.1016/j.jseaes.2023.105736

After the strikingly similar onset of the Aptian Cretaceous sedimentation in terms of facies and depositional environments, suggesting a wide epeiric sea, a major differentiation is observed in the three studied areas since the Aptian–Albian boundary, when erosion, deepening, and the formation of hardgrounds, with local, asynchronous and episodic reprise of shallow-water carbonate sedimentation is documented. This change in the stratigraphic evolution, in places where previous (Aptian) sedimentation was homogeneous, suggests a tectonic differentiation in domains characterized by different stratigraphic evolution. This scenario reflects a major geodynamic re-organization that will led to the opening of the deep-water Late Cretaceous seaways, today documented by the complex arrangement of ophiolitic belts, mostly interpreted as evidence of back-arc basins, later closed by the convergence related to the closure of the Neotethys Ocean between the end of the Cretaceous and the Paleogene. The stratigraphic study and comparison of the selected Cretaceous successions indicate that the Aptian–Albian boundary interval represents a turning point in the geological evolution of Iran, marking the rapid transition from a tectonically quiet epicontinental domain to an area strongly affected by extensional tectonics taking to the opening of oceanic seaways.

Further integrated multidisciplinary studies on Cretaceous successions of Iran are expected to improve our knowledge of the Late Mesozoic to Cenozoic history of the Iranian blocks, defining the timing and distribution of the different evolution recorded in the various domains that were identified in this area after the Cimmerian events.

Acknowledgements

We would like to thank the Geological Survey of Iran (GSI) for support in the organization of fieldwork, as well as Mattia Nembrini and Gabriel Quemada (University of Milano) for support during field work. The detailed and constructive comments of three anonymous reviewers and of the Editor are here warmly thanked: they helped us to improve the original manuscript. We would like to acknowledge the Darius Project for funding our research.

References

Abad, M. T. K., Schlagintweit, F., Vaziri, S. H., Aryaei, A. A., Ashouri, A. R., 2013. Balkhania balkhanica MAMONTOVA, 1966 (benthic foraminifera) and Kopetdagaria sphaerica MASLOV, 1960 (dasycladalean alga) from the Lower Cretaceous Tirgan Formation of the Kopet Dagh mountain range (NE Iran) and their paleobiogeographic significance. Facies, 59(1), 267–285.

Agard, P., Omrani, J., Jolivet, L., Mouthereau, F., 2005. Convergence history across Zagros (Iran): constraints from collisional and earlier deformation. International Journal of Earth Sciences, 94(3), 401–419.

Alavi, M., 1991. Sedimentary and structural characteristics of the Paleo-Tethys remnants in northeastern Iran. Geological Society of American Bulletin, 103, 983–992.

https://doi.org/10.1016/j.jseaes.2023.105736

Alavi, M., Vazir, H., Seyed-Emami, K., Lasemi, Y., 1997. The Triassic and associated rocks of the Nakhlak and Aghdarband areas in central and northeastern Iran as remnants of the southern Turanian active continental margin. Geological Society of America Bulletin, 109, 1563–1575.

Angiolini, L., Gaetani, M., Muttoni, G., Stephenson, M.H., Zanchi, A. 2007. Tethyan oceanic currents and climate gradients 300 m.y. ago. Geology, 35, 1071–1074.

Arnaud-Vanneau, A., and Schroeder, R., 1976. Paleodictyoconus actinostoma n. sp. Orbitolinidae nouveau des “Couches á orbitolines” intra-urgoniennes du Vercors (France). Géobios, 9 (3), 279–289.

Babaahmadi, A., Davoudian, A. R., Mohajjel, M., 2021. Transpression in the Sanandaj–Sirjan Zone (Zagros Orogen, Iran) during the Jurassic and Early Cretaceous: Evidence from the North Shahrekord Shear Zone. Journal of Structural Geology, 149, 104387.

Balini, M., Nicora, A., Berra, F., Garzanti, E., Levera, M., Mattei, M., Muttoni, G., Zanchi, A., Bollati, I., Larghi, C. and Zanchetta, S., 2009. The Triassic stratigraphic succession of Nakhlak (Central Iran), a record from an active margin. Geological Society, London, Special Publications, 312(1), 287–321.

Badertscher, N., P., Burkhard, M., 2000. Brittle-ductile deformation in the Glarus thrust Lochseiten (LK) calc-mylonite. Terra Nova, 12, 281–288.

Bagheri, S., Stampfli, G.M., 2008. The Anarak, Jandaq and Posht-e-Badam metamorphic complexes in central Iran: new geological data, relationships and tectonic implications. Tectonophysics, 451(1-4), 123–155.

Barrier, E., Vrielynck, B., 2008. Palaeotectonic map of the Middle East, Atlas of 14 maps, tectonosedimentary-palinspastic maps from Late Norian to Pliocene. Commission for the Geologic Map of the World (CCMW, CCGM), Paris, France.

Barrier, E., Vrielynck, B., Brouillet, J.F., Brunet, M.F., 2018. Paleotectonic Reconstruction of the Central Tethyan Realm. Tectonono-Sedimentary-Palinspastic maps from Late Permian to Pliocene. Atlas of 20 maps (scale: 1:15.000.000). CCGM/CGMW, Paris, http://www.ccgm.org.

Baumfalk, Y. A., 1986. The evolution of Orbitoides media (Foraminiferida) in the Late Campanian. The Journal of Foraminiferal Research, 16, 293–312.

Baumfalk, Y.A., van Hinte, J.E., 1985. Orbitoides media (D’ARCHIAC) in the Campanian deposits of the A 10 motorway at Mirambeau (Charente maritime). Cretaceous Research, 6, 81–189.

Berberian, M., King, G., 1981. Toward a paleogeography and tectonic evolution of Iran. Canadian Journal of Earth Science, 18, 210–265.

Berra, F., Zanchi, A., Angiolini, L., Vachard, D., Vezzoli, G., Zanchetta, S., Bergomi, M., Javadi, H.R., Kouhpeyma, M., 2017. The upper Palaeozoic Godar-e-Siah Complex of Jandaq: evidence and significance of a North Palaeotethyan succession in Central Iran. Journal of Asian Earth Sciences, 138, 272–290.

Berra, F., Zanchi, A., Mattei, M., Nawab, A., 2007. Late Cretaceous transgression on a Cimmerian high (Neka Valley, Eastern Alborz, Iran): A geodynamic event recorded by glauconitic sands. Sedimentary Geology, 199(3-4), 189–204.

Boulin, J., 1991. Structures in Southwest Asia and evolution of the eastern Tethys. Tectonophysics, 196, 211-–268.

Breistroffer, M., 1947. Sur les zones d’Ammonites dans l’Albien de France et d’Angleterre. Travaux du Laboratoire de Géologie de la Faculté des Sciences de Grenoble, 26, 1–88.

Carter, R.M., 1968. Functional studies on the Cretaceous oyster Arctostrea. Palaeontology, 11, 3, 458–485.

Chiocchini, M., Chiocchini, R.A., Didaskalou, P., Potetti, M., 2008. Micropaleontological and biostratigraphical researches on the Mesozoic of the Latium-Abruzzi carbonate platforms (Central Italy). Memorie Descrittive della Carta Geologicad'Italia, 84, 63.

Davies, R.B., Casey, D.M., Horbury, A.D., Sharland, P.R., Simmons, M.D., 2002. Early to mid-Cretaceous mixed carbonate-clastic shelfal systems: Examples, issues, and models from the Arabian Plate. GeoArabia, 7, 3, 541–598.

https://doi.org/10.1016/j.jseaes.2023.105736

Davoudian A.R., Genser J. Neubauer F., Shabanian N., 2016. 40Ar/39Ar mineral ages of eclogites from North Shahrekord in the Sanandaj–Sirjan Zone, Iran: Implications for the tectonic evolution of Zagros orogen. Gondwana Research 37, 216–240.

Dercourt, J., Zonenshain, L.P., Ricou, L.E., Kazmin, V.G., Le Pichon, X., Knipper, A.L., Grandjacquet, C., Sbortshikov, I.M., Geyssant, J., Lepvrier, C., Pechersky, D.H., 1986. Geological evolution of the Tethys belt from the Atlantic to the Pamirs since the Lias. Tectonophysics, 123, 241–315.

Dercourt, J., Gaetani, M., Vrielynck, B., Barrier, E., Biju-duval, B., Brunet, M.F., Cadet, J. P., Crasquin, S., Sandulescu, M., 2000. Atlas Peri-Tethys, Palaeogeographical Maps. Explanatory notes, I-XX+269 pp., and 24 maps. CCGM/CGMW, Paris.

Dunham, R.J., 1962. Classification of carbonate rocks according to depositional texture. In: Classification of Carbonate Rocks (Ed. Ham, W.E.), AAPG Mem., 1, 108–121.

Embry, A.F. III,Klovan, J.S., 1971. A Late Devonian reef tract on north-eastern Banks Island, NWT. Bullettin of Canadian Petroleum Geology, 4, 730–781.

Farbod, Y., Bellier, O., Shabanian, E., Abbassi, M. R., 2011. Geomorphic and structural variations along the Doruneh Fault System (central Iran). Tectonics, 30, TC6014, doi:10.1029/2011TC002889.

Flügel, E., 2004. Microfacies of Carbonate Rocks. Analysis, Interpretation and Application. Springer, Berlin, 984 pp.

Fluteau, F., Ramstein, G., Besse, J., Guiraud, R., Masse, J. P., 2007. Impacts of palaeogeography and sea level changes on Mid-Cretaceous climate. Palaeogeography, Palaeoclimatology, Palaeoecology, 247, 357–381.

Frau, C., Tendil, A. J. B., Pohl, A., Lanteaume, C., 2020. Revising the timing and causes of the Urgonian rudistid-platform demise in the Mediterranean Tethys. Global and Planetary Change, 187, 103124.

Freneix, S., Viaud, J.-M., 1986. Huîtres du Crétacé supérieur du basin de Challans-Commequiers (Vendée). Biostratigraphie, taxinomie, paléobiologie. - Bulletin Trimestrielde la Société Géologiquede Normandie et Amis du Muséum du Havre, 73, 13–79.

Gale, A.S., Mutterlose, J., Batenburg, S., Gradstein, F.M., Agterberg, F.P., Ogg, J.G. Petrizzo, M.R., 2020. The cretaceous period. In Geologic time scale 2020 (pp. 1023–1086). Elsevier.

Ghasemi, A., Talbot, C. J., 2006. A new tectonic scenario for the Sanandaj–Sirjan Zone (Iran). Journal of Asian Earth Sciences, 26, 683–693.

Gheiasvand, M., Föllmi, K. B., Stampfli, G. M., Vérard, C., Luciani, V., Morsilli, M., 2021. Paleoenvironment and paleobiogeography of Lower Cretaceous carbonate successions of the northern Tethyan margin: Examples from Northeastern and Central Iran. Journal of Asian Earth Sciences, 213, 104752.

Gyomlai, T., Agard, P., Jolivet, L., Larvet, T., Bonnet, G., Omrani, J., Larson, K., Caron, J., Noël, J., 2022. Cimmerian metamorphism and post Mid-Cimmerian exhumation in Central Iran: Insights from in-situ Rb/Sr and U/Pb dating. Journal of Asian Earth Sciences, 233, 105242. doi: https://doi.org/10.1016/j.jseaes.2022.105242Hairapetian, V., Wilmsen, M., Ahmadi, A., Shojaei, Z., Berensmeier, M., Majidifard, M. R., 2018. Integrated stratigraphy, facies analysis and correlation of the upper Albian–lower Turonian of the Esfahan area (Iran): unravelling the conundrum of the so-called “Glauconitic Limestone”. Cretaceous Research, 90, 391-–411.

Haq, B.U., 2014. Cretaceous eustasy revisited. Global and Planetary Change, 113, 44–58.

Hassanzadeh, J., Wernicke, B.P., 2016. The Neotethyan Sanandaj–Sirjan zone of Iran as an archetype for passive margin-arc transitions. Tectonics 35, 586–621.

Hay, W.W., 2008. Evolving ideas about the Cretaceous climate and ocean circulation. Cretaceous Research 29, 725–753.

Hay, W.W., Floegel, S., 2012. New thoughts about the Cretaceous climate and oceans. Earth Science Review 115 (4), 262–272. http://dx.doi.org/10.1016/j.earscirev.2012.09.008.

Hu, X., Wagreich, M., Yilmaz, I. O., 2012. Marine rapid environmental/climatic change in the Cretaceous greenhouse world. Cretaceous Research, 38, 1–6.

Huber, B.T., Petrizzo, M.R., Young, J., Falzoni, F., Gilardoni, S., Bown, P.R., Wade, B.S., 2016. A new online taxonomic database for planktonic foraminifera. Micropaleontology 62, 429–438.

Jablonsky, D., Lutz, R.A., 1980. Molluscan larval shell morphology. Ecological and paleontological applications. In: Rhoads D.C. and R.A. LUTZ, Eds., Skeletal growth of aquatic organisms. New York and London, 323–377.

Jarvis, I., Mabrouk, A., Moody, R. T., de Cabrera, S., 2002. Late Cretaceous (Campanian) carbon isotope events, sea-level change and correlation of the Tethyan and Boreal realms. Palaeogeography, Palaeoclimatology, Palaeoecology, 188, 215–248.

Javadi, H. R., Ghassemi, M. R., Shahpasandzadeh, M., Guest, B., Ashtiani, M. E., Yassaghi, A., Kouhpeyma M., 2013. History of faulting on the Doruneh Fault System: implications for the kinematic changes of the Central Iranian Microplate. Geological Magazine, 150, 651–672.

Javadi, H. R., Esterabi Ashtiani, M., Guest, B., Yassaghi, A., Ghassemi, M. R., Shahpasandzadeh, M., Naeimi, A., 2015. Tectonic reversal of the western Doruneh Fault System: Implications for Central Asian tectonics. Tectonics, 34, 2034–2051.

Jentzer, M., Agard, P., Bonnet, G., Monié, P., Fournier, M., Whitechurch, H., Omrani, J., Zarrinkoub, M.H., Khatib, M.M., Kohansal, R., Do Couto, D., 2022. The North Sistan orogen (Eastern Iran): Tectono-metamorphic evolution and significance within the Tethyan realm. Gondwana Research 109, 460–492.

Kazemi, Z., Ghasemi, H., Tilhac, R., Griffin, W., Moghadam, H. S., O'Reilly, S., Mousivand, F., 2019. Late Cretaceous subduction-related magmatism on the southern edge of Sabzevar basin, NE Iran. Journal of the Geological Society, 176, 530–552.

Lindenberg, H.G., Gorler, K., Ibbeken, H., 1983. Stratigraphy, structure and orogenetic evolution of the Sabzevar Zone in the area of Oryan, Khorasan, NE Iran. Geological Survey of Iran, 51, 119–143

Mancinelli, A., Chiocchini, M., 2006. Cretaceous benthic foraminifers and calcareous algae from Monte Cairo (southern Latium, Italy). Bollettino della Società Paleontologica Italiana, 45, 91–113.

Masse, J.-P., 2003. Integrated stratigraphy of the lower Aptian and applications to carbonate platforms: a state of the art. In: Gili E. et al. (eds) North Africa Cretaceous carbonate platform systems, Kluver Academic Publishers, Amsterdam, 203–214.

Mattei, M., Cifelli, F., Muttoni, G., Rashid, H., 2015. Post-Cimmerian (Jurassic-Cenozoic) paleogeography and vertical axis tectonic rotations of Central Iran and the Alborz Mountains. Journal of Asian Earth Sciences, 102, 92–101. https://doi.org/10.1016/j. jseaes.2014.09.038

Miller, K. G., Kominz, M. A., Browning, J. V., Wright, J. D., Mountain, G. S., Katz, M. E., Sugarman, P.J., Cramer, B.S., Christie-Blick, N., Pekar, S. F. 2005. The Phanerozoic record of global sea-level change. Science, 310(5752), 1293–1298.

Moghadam, H. S. Stern, R. J., 2021. Subduction initiation causes broad upper plate extension: The Late Cretaceous Iran example. Lithos, 398, 106296.

Moghadam, H. S., Corfu, F., Chiaradia, M., Stern, R. J., Ghorbani, G., 2014. Sabzevar Ophiolite, NE Iran: Progress from embryonic oceanic lithosphere into magmatic arc constrained by new isotopic and geochemical data. Lithos, 210, 224–241.

Moghadam, H. S., Li, Q. L., Griffin, W. L., Chiaradia, M., Hoernle, K., O'Reilly, S. Y., Esmaeili, R., 2021. The Middle-Late Cretaceous Zagros ophiolites, Iran: Linking of a 3000 km swath of subduction initiation fore-arc lithosphere from Troodos, Cyprus to Oman. GSA Bulletin, 134, 1414–1442.

Mohajjel, M., Fergusson, C. L., Sahandi, M. R., 2003. Cretaceous–Tertiary convergence and continental collision, Sanandaj–Sirjan zone, western Iran. Journal of Asian Earth Sciences, 21, 397–412.

Monsef, I., Zhang, Z., Shabanian, E., le Roux, P., Rahgoshay, M., 2022. Tethyan subduction and Cretaceous rift magmatism at the southern margin of Eurasia: Evidence for crustal evolution of the South Caspian Basin. Earth-Science Reviews, 228, 104012.

Moullade, M., Granier, B., Tronchetti, G., 2011. The Aptian stage: Back to fundamentals. Episodes Journal of International Geoscience, 34, 148–156.

https://doi.org/10.1016/j.jseaes.2023.105736

Niechwedowicz, M., Walaszczyk, I., Barski, M., 2021. Phytoplankton response to palaeoenvironmental changes across the Campanian–Maastrichtian (Upper Cretaceous) boundary interval of the Middle Vistula River section, central Poland. Palaeogeography, Palaeoclimatology, Palaeoecology, 577, 110558.

Omrani, H., Moazzen, M., Oberhänsli, R., Altenberger, U., Lange, M., 2013. The Sabzevar blueschists of the North-Central Iranian micro-continent as remnants of the Neotethys-related oceanic crust subduction. International Journal of Earth Sciences, 102, 1491–1512.

Özcan, E., Yücel, A.O., Catanzariti, R., Kayğılı, S., Okay, A.I., Simmons, M.D., Pignatti, J., Abbasi, I.A., Erbil, Ü., 2021. Multiple *Orbitoides* D’Orbigny lineages in the Maastrichtian? Data from the Central Sakarya Basin (Turkey) and Arabian Platform successions (Southeastern Turkey and Oman). Swiss Journal Palaeontology 140, 8.

Petrizzo, M.R., Huber, B.T., Falzoni, F., MacLeod, K.G., 2020. Changes in biogeographic distribution patterns of southern mid-to high latitude planktonic foraminifera during the Late Cretaceous hot to cool greenhouse climate transition. Cretaceous Research, 115, 104547.

Pirnia, T., Saccani, E., Torabi, G., Chiari, M., Goričan, Š., Barbero, E., 2020. Cretaceous tectonic evolution of the Neo-Tethys in Central Iran: Evidence from petrology and age of the Nain-Ashin ophiolitic basalts. Geoscience Frontiers, 11, 57–81.

Premoli Silva, I., Sliter, W.V., 1994. Cretaceous planktonic foraminiferal biostratigraphy and evolutionary trends from the Bottaccione section, Gubbio, Italy. Palaeontographia italica, 82, 1–89.

Rahmati-Ilkhchi, M., Jeřábek P., Faryad, S.W., Koyi, H.A., 2011. Mid-Cimmerian, Early Alpine and Late Cenozoic orogenic events in the Shotur Kuh metamorphic complex, Great Kavir block, NE Iran. Tectonophysics 494, 101–117.

Raisossadat, S. N., Latil, J. L., Hamdani, H., Jaillard, E., Amiribakhtiar, H., 2021. The Kazhdumi Formation (Lower Cretaceous, upper Aptian–upper Albian) in the Zagros Basin, Iran. Cretaceous Research, 127, 104920.

Robaszynski, F., Caron, M., 1995. Cretaceous planktonic foraminifera: comments on the Europe-Mediterranean zonation. Bulletin de la Société Géologique de France, 166, 681–692.

Robert, A. M., Letouzey, J., Kavoosi, M. A., Sherkati, S., Müller, C., Vergés, J., Aghababaei, A., 2014. Structural evolution of the Kopeh Dagh fold-and-thrust belt (NE Iran) and interactions with the South Caspian Sea Basin and Amu Darya Basin. Marine and Petroleum Geology, 57, 68–87.

Romanko, E., 1969. Mesr 6957 and Arusan 7059 sheets of the geological map of Iran at 1: 100,000 scale.

Rossetti, F., Nasrabady, M., Vignaroli, G., Theye, T., Gerdes, A., Razavi, M.H., Vaziri, H.M., 2010. Early Cretaceous migmatitic mafic granulites from the Sabzevar range (NE Iran): implications for the closure of the Mesozoic peri-Tethyan oceans in central Iran. Terra Nova, 22, 26–34.

Rothman, D. H., 2002. Atmospheric carbon dioxide levels for the last 500 million years. Proceedings of the National Academy of Sciences, 99, 4167–4171.

Ruttner, A.W. 1993. Southern borderland of Triassic Laurasia in north-east Iran. Geologische Rundschau, 82, 110–120.

Sames, B., Wagreich, M., Wendler, J. E., Haq, B. U., Conrad, C. P., Melinte-Dobrinescu, M. C., Hu, X., Wendler I., Wolfgring, E., Yilmaz, I.Ö., Zorina, S. O., 2016. Short-term sea-level changes in a greenhouse world–A view from the Cretaceous. Palaeogeography, Palaeoclimatology, Palaeoecology, 441, 393–411.

Schlagintweit, F., Rashidi, K., 2022. The “Orbitolina Limestone” of central Iran: new data about microfacies, orbitolinid biostratigraphy, and palaeogeography. Facies, 68, 1–15.

Schlagintweit, F., Bucur I.I., Rashidi, K., Saberzadeh, B., 2013a. Praeorbitolina claveli n. sp. (benthic foraminifera) from the lower Aptian (Bedoulian) of Central Iran. Carnets de Géologie/Notebooks on Geology, Letter 2013/04 (CH2013_L04), 255–272.

Schlagintweit, F., Bucur I.I., Rashidi, K., Hanifzadeh, R., 2013b. Torremiroella hispanica BRUN AND CANEROT, 1979 (benthic foraminifera) from the Lower Cretaceous of Central Iran and its palaeobiogeographic significance. Cretaceous Research, 46, 272–279.

https://doi.org/10.1016/j.jseaes.2023.105736

Schlanger, S. O., Jenkyns, H. C. (1976). Cretaceous oceanic anoxic events: causes and consequences. Geologie en Mijnbouw, 55, 179–184.

Schroeder, R., 1965. *Dictyoconus pachymarginalis* n. sp. aus dem Apt des Alburz Gebirges (Nord-Iran (Studien über primitive Orbitolinidae III). Eclogae Geologicae Helvetiae, 58, 975–980.

Schroeder, R., van Buchem F.S.P., Cherchi, A., Baghbani, D., Vincent, B., Immenhauser, A., Granier, B., 2010. Revised orbitolinid biostratigraphic zonation from the Barremian-Aptian of the eastern Arabian Plate and implications for regional stratigraphic correlations. GeoArabia Special Publication 4, 49–96.

Şengör, A.M.C. 1979. Mid-Mesozoic closure of Permo-Triassic Tethys and its implications. Nature, 279, 590–593.

Şengör, A.M.C. 1984. The Cimmeride orogenic system and the tectonics of Eurasia. Geological Society of America Special Paper, 195, 1–74.

Şengör, A.M.C. 1990. A new model for the late Palaeozoic-Mesozoic tectonic evolution of Iran and implications for Oman. In: Robertson, A. H., Searle M. P. and Ries A.C. (eds). The Geology and tectonics of the Oman region. Geological Society Special Publication, 49, 797–831.

Shakerardakani, F., Neubauer, F., Liu, X., Dong, Y., Monfaredi, B., Li, X.H., 2021. New detrital zircon U–Pb insights on the palaeogeographic origin of the central Sanandaj–Sirjan zone, Iran. Geological Magazine, 158, 2165–2186.

Shakerardakani F., Neubauer F., Bernroider M., Finger F., Hauzenberger C., Genser J., Waitzinger M., Monfaredi B., 2022. Metamorphic stages in mountain belts during a Wilson cycle: A case study in the central Sanandaj–Sirjan zone (Zagros Mountains, Iran) Geoscience Frontiers, 13, 101272.

Sharafi, M., Rodríguez-Tovar, F. J., Janočko, J., Bayet-Goll, A., Mohammadi, M., Khanehbad, M., 2021. Environmental significance of trace fossil assemblages in a tide–wave-dominated shallow-marine carbonate system (Lower Cretaceous), northern Neo-Tethys margin, Kopet-Dagh Basin, Iran. International Journal of Earth Sciences, 111, 103–126.Sharland, P.R., Archer, R., Casey, D.M., Davis, R.B., Hall, S.H., Heward, A.P., Horbury A.D., Simmons, M.D. 2001. Arabian Plate sequence stratigraphy. GeoArabia Special Publication no. 2, Gulf PetroLink, Bahrain, 371 pp.

Sheikholeslami, M. R., Kouhpeyma, M., 2012. Structural analysis and tectonic evolution of the eastern Binalud Mountains, NE Iran. Journal of Geodynamics, 61, 23–46. https://doi.org/10.1016/j.jog.2012.06.010

Sheikholeslami, M. R., Oberhansli, R., Ghassemi, M. R., 2019. Transpression tectonics in the eastern Binalud Mountains, northeast Iran; Insight from finite strain analysis, vorticity and 40Ar/39Ar dating. Journal of Asian Earth Sciences, 179, 219–237. https://doi.org/10.1016/j.jseaes.2019.04.014

Shojaat,B., Hassanipak, A.A.,Mobasher, K., Ghazi, A.M., 2003. Petrology, geochemistry and tectonics of the Sabzevar ophiolite, North Central Iran. Journal of Asian Earth Sciences, 21, 1053–1067

Sloss, L.L. (1963) Sequences in Cratonic Interior of North America. Geological Society of America Bulletin, 74, 93–114.

Spicer, R. A., Corfield, R. M., 1992. A review of terrestrial and marine climates in the Cretaceous with implications for modelling the 'Greenhouse Earth'. Geological Magazine, 129, 169–180.

Stampfli, G.M., Borel, G.D., 2002. A plate tectonic model for the Paleozoic and Mesozoic constrained by dynamic plate boundaries and restored synthetic oceanic isochrons. Earth and Planetary ScienceLetters, 196, 17–33.

Stöcklin, J. 1974. Possible ancient continental margins in Iran. In: Burk, C.A. and Drake, C.L. (eds). The geology of Continental Margins, 873–887.

Stöcklin, J., 1981. A brief report on geodynamics in Iran. Zagros Hindu Kush Himalaya Geodynamic Evolution, 3, 70–74.

Tadayon, M., Rossetti, F., Zattin, M., Calzolari, G., Nozaem, R., Salvini, F., Faccenna, C., Khodabakhshi, P., 2019. The long-term evolution of the Doruneh Fault region (Central Iran): A key to understanding the spatio-

https://doi.org/10.1016/j.jseaes.2023.105736

temporal tectonic evolution in the hinterland of the Zagros convergence zone. Geological Journal, 54, 1454–1479.

Tirrul, R., Bell, I.R., Griffis, R.J., Camp, V.E., 1983. The Sistan suture zone of eastern Iran. Geological Society of America Bulletin, 94, 134–150.

Torabi, G., 2009. Chromitite potential in mantle peridotites of the Jandaq ophiolite (central Iran). Comptes Rendus Geoscience, 341, 982–992. https://doi.org/10.1016/j.crte.2009.07.014

van Buchem, F. S., Al-Husseini, M. I., Maurer, F., Droste, H. J., Yose, L. A., 2010. Sequence-stratigraphic synthesis of the Barremian–Aptian of the eastern Arabian Plate and implications for the petroleum habitat. Barremian-Aptian stratigraphy and hydrocarbon habitat of the eastern Arabian Plate. GeoArabia Special Publication, 4, 9–48.

Vaziri, S. H., Senowbari-Daryan, B., & Kohansal Ghadimvand, N., 2005. Lithofacies and microbiofacies of the Upper Cretaceous rocks (Sadr unit) of Nakhlak area in Northeastern Nain, Central Iran. Journal of Geosciences-Osaka City University, 48, 71.

Vaziri, S. H., Fürsich, F. T., & Kohansal-Ghadimvand, N., 2012. Facies analysis and depositional environments of the Upper Cretaceous Sadr unit in the Nakhlak area, Central Iran. Revista mexicana de ciencias geológicas, 29, 384–397.

Velić, I., 2007. Stratigraphy and Palaeobiogeography of Mesozoic Benthic Foraminifera of the Karst Dinarides (SE Europe). Geologia Croatica 60, 1–60.

Viaretti M., Crippa G., Posenato R., Shen S., Angiolini L., 2021. Lopingian brachiopods from the Abadeh section (Central Iran) and their biostratigraphic implications. Bollettino della Società Paleontologica Italiana, 60, 213–254. doi: 10.4435/BSPI.2021.16

Wagreich, M., Lein, R., Sames, B., 2014. Eustasy, its controlling factors, and the limnoeustatic hypothesis – concepts inspired by Eduard Suess. Austrian Journal of Earth Sciences 107, 115–131.

Wilmsen, M., Wiese, F., Seyed-Emami, K. & Fürsich, F.T. (2005): First record and significance of Cretaceous (Turonian) ammonites from the Shotori Mountains, east-central Iran. - Cretaceous Research, 26, 181–195.

Wilmsen, M., Fürsich, F. T., Seyed-Emami, K., Majidifard, M. R., Taheri, J., 2009. The Cimmerian Orogeny in northern Iran: Tectono-stratigraphic evidence from the foreland. Terra Nova, 21, 211–218.

Wilmsen, M., Fürsich, F. T., Seyed-Emami, K., Majidifard, M. R., & Zamani-Pedram, M., 2010. Facies analysis of a large-scale Jurassic shelf-lagoon: the Kamar-e-Mehdi Formation of east-central Iran. Facies, 56, 59–87.

Wilmsen, M., Fürsich, F. T., Majidifard, M. R., 2013. The Shah Kuh Formation, a latest Barremian–Early Aptian carbonate platform of Central Iran (Khur area, Yazd Block). Cretaceous Research, 39, 183–194.

Wilmsen, M., Fürsich, F. T., Majidifard, M. R., 2015. An overview of the Cretaceous stratigraphy and facies development of the Yazd Block, western Central Iran. Journal of Asian Earth Sciences, 102, 73-–91.

Wilmsen, M., Berensmeier, M., Fürsich, F. T., Majidifard, M. R., Schlagintweit, F., 2018a. A Late Cretaceous epeiric carbonate platform: the Haftoman Formation of central Iran. Facies, 64, 1–24.

Wilmsen, M., Storm, M., Fürsich, F. T., Majidifard, M. R., Schlagintweit, F., Hart, M., 2018b. The mid-Cretaceous Debarsu Formation (Upper Albian–Middle Turonian) of Central Iran: Depositional environment, palaeogeography, and sequence stratigraphic significance. Facies, 64, 1–28.

Wilmsen, M., Berensmeier, M., Fürsich, F. T., Schlagintweit, F., Hairapetian, V., Pashazadeh, B., Majidifard, M. R., 2020. Mid-Cretaceous biostratigraphy (ammonites, inoceramid bivalves and foraminifers) at the eastern margin of the Anarak Metamorphic Complex (Central Iran). Cretaceous Research, 110, 104411.

Wilmsen, M., Fürsich, F.T., Seyed-Emami, K. & Majidifard, M.R. (2021): The Upper Jurassic Garedu Red Bed Formation of the northern Tabas Block: elucidating Late Cimmerian tectonics in east-Central Iran. - International Journal of Earth Sciences, 110, 767–790.

Wilmsen, M., Fürsich, F. T., Majidifard, M. R., 2022. Youngest Cretaceous dinosaur tracksite from the Middle East (Maastrichtian, Farrokhi Formation, Central Iran). Palaeobiodiversity and Palaeoenvironments, 102, 437–447.

Yao, H., Chen, X., Brunner, B., Birgel, D., Lu, Y., Guo, H., Wang, C., Peckmann, J., 2022. Hydrocarbon seepage in the mid-Cretaceous greenhouse world: A new perspective from southern Tibet. Global and Planetary Change, 208, 103683.

Yazdi-Moghadam, M., Parandavar, M., Sarfi, M., Sharifi, M., 2021. Integrated biostratigraphy (orbitolinids and calcareous nannofossils) of the Lower Cretaceous Taft Formation in Isfahan, Central Iran. Cretaceous Research, 126, 104918.

Zanchi, A., Berra, F., Mattei, M., Ghassemi, M., Sabouri, J., 2006. Inversion tectonics in central Alborz, Iran. Journal of Structural Geology, 28, 2023–2037. doi: 10.1016/j.jsg.2006.06.020.

Zanchi, A., Berra, F., Mattei, M., Zanchetta, S., Nawab, A., Sabouri, J., 2005. The early Mesozoic Cimmerian orogeny in the Alborz mountains, Iran. Geophysical Research Abstract, 7, 1607–7962.

Zanchi, A., Zanchetta, S., Berra, F., Mattei, M., Garzanti, E., Molyneux, S., Nawab, A., Sabouri, J. 2009a. The Eo-Cimmerian (Late? Triassic) orogeny in North Iran. Geological Society, London, Special Publications, 312, 31–55.

Zanchi, A., Zanchetta, S., Garzanti, E., Balini, M., Berra, F., Mattei, M., Muttoni, G., 2009b. The Cimmerian evolution of the Nakhlak-Anarak area, central Iran, and its bearing for the reconstruction of the history of the Eurasian margin. In: M.F. Brunet, M. Wilmsen, and J.W. Granath (Eds.), South Caspian to Central Iran Basins. Geological Society, London, Special Publications, 312, 261–286.

Zanchi, A., Malaspina, N., Zanchetta, S., Berra, F., Benciolini, L., Bergomi, M., Cavallo A., Javadi, H., R., Kouhpeyma, M. (2015). The Cimmerian accretionary wedge of Anarak, Central Iran. Journal of Asian Earth Sciences, 102, 45–72.

Zanchi, A., Zanchetta, S., Berra, F., Mattei, M., Javadi, H. R., Montemagni, C., 2021. Cenozoic Dextral Shearing Along the Arusan Sector of the Great Kavir–Doruneh Fault System (Central Iran). Tectonics, 40, e2021TC006766.

Figure captions

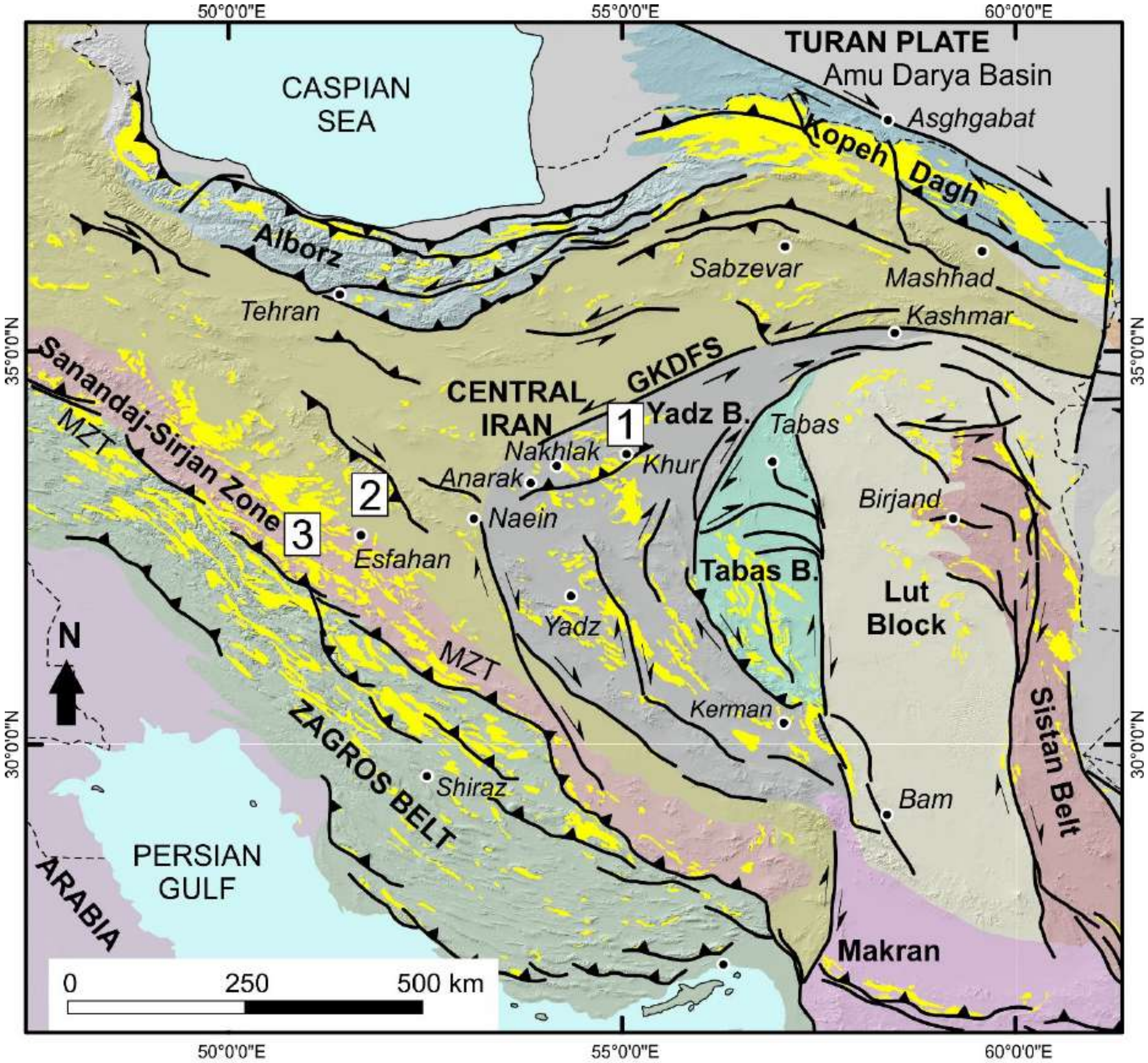

Fig. 1 – Distribution of Cretaceous outcrops in the domains of Iran, with the position of the studied areas. 1=Arousan; 2=Esfahan north; 3=Tiran. In yellow the Cretaceous outcrops in the different Iranian domains. MTZ: Main Zagros Thrust; GKDFS: Great Kavir-Doruneh Fault System.

https://doi.org/10.1016/j.jseaes.2023.105736

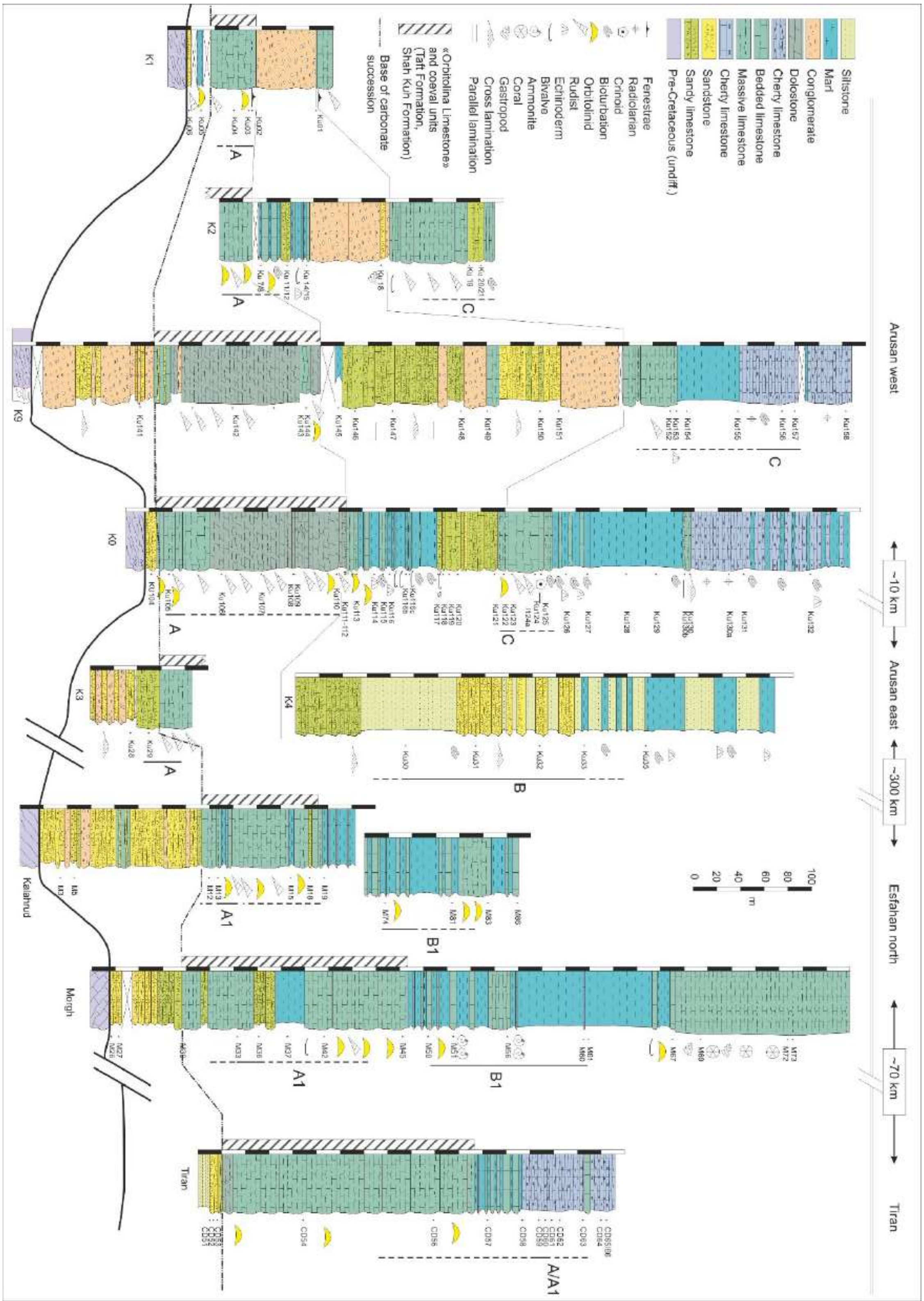

Fig. 2 – Simplified stratigraphic logs of the studied successions. Log coordinates: K1= 33°59'14", 54°40'47"; K9= 34°03'13", 54°55'18"; K3: 34°09'06", 55°11'20"; K4: 34°08'53", 55°10'57"; K0: 34°08'02", 55°05',07"; K2: 33°55'31", 54°45'40"; Morgh= 33°02'42", 51°52'12"; Kalahrood: 33°22'18", 51°22'37"; Tiran: 32°44'14", 51°12'40". Letters A, A1, B, B1 and C mark the stratigraphic distribution of the foraminiferal assemblages described in the text.

https://doi.org/10.1016/j.jseaes.2023.105736

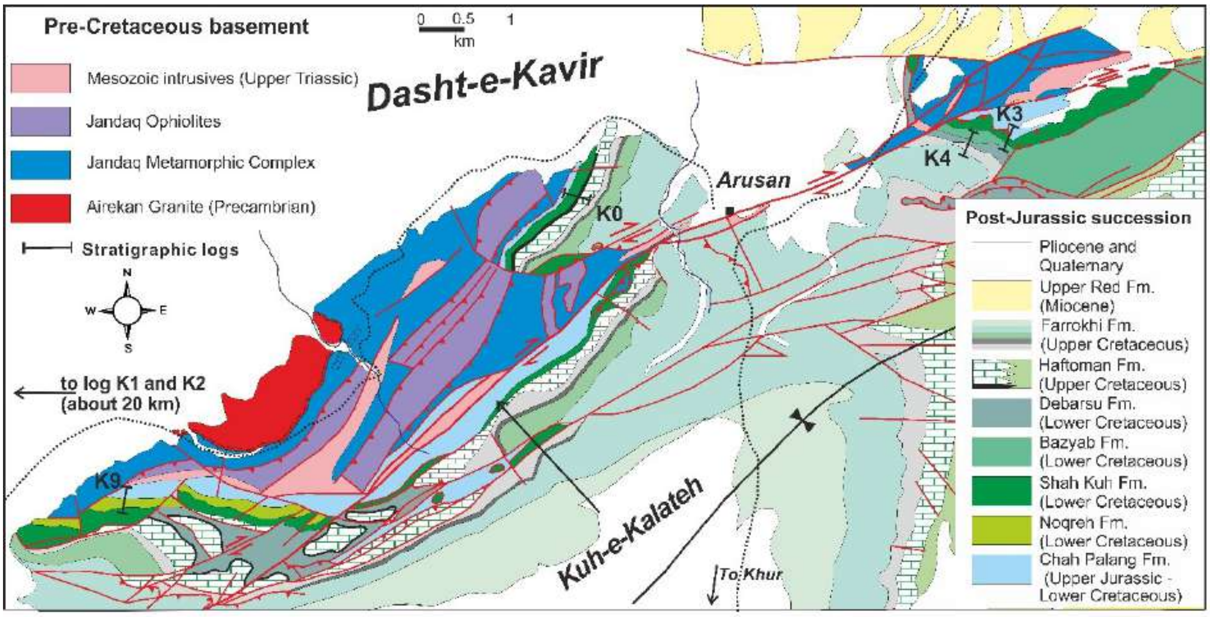

Fig. 3 - Simplified geological setting of the Arusan area, compiled from existing geological maps and new surveys.

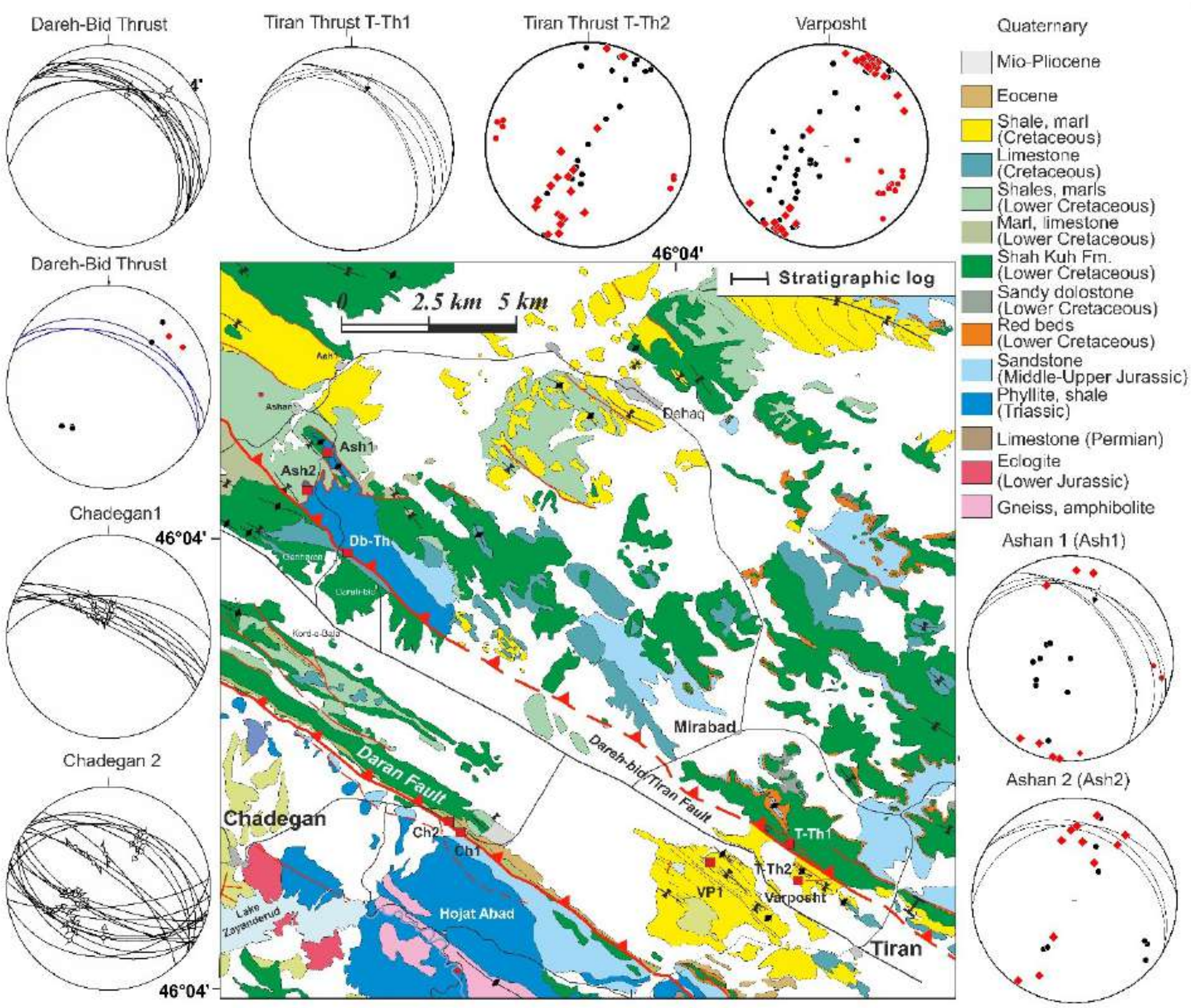

Fig. 4 Simplified geological setting of the Tiran area, compiled from existing geological maps and new surveys, including original structural data.

https://doi.org/10.1016/j.jseaes.2023.105736

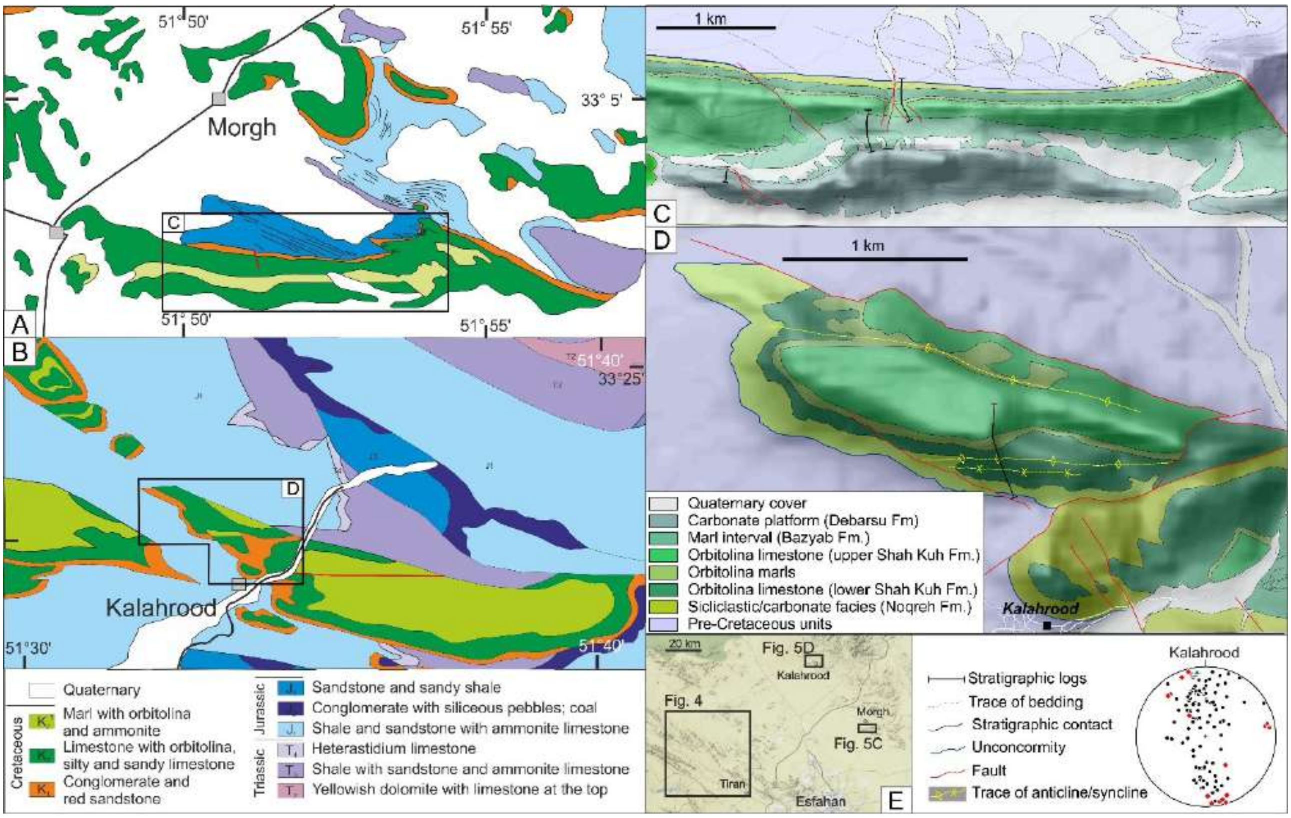

Fig. 5 - Geological maps redrawn from the sheet 1:100.000 "Tarq" of the geological map of Iran for the area of Morgh (A) and Kalahrood (B), the boxes with the letters C and D refers to the preliminary geological maps of Morgh (C) and Kalahrood, with structural data (D); in (E) the geographic position of the Tiran, Morgh and Kalahrood areas.

https://doi.org/10.1016/j.jseaes.2023.105736

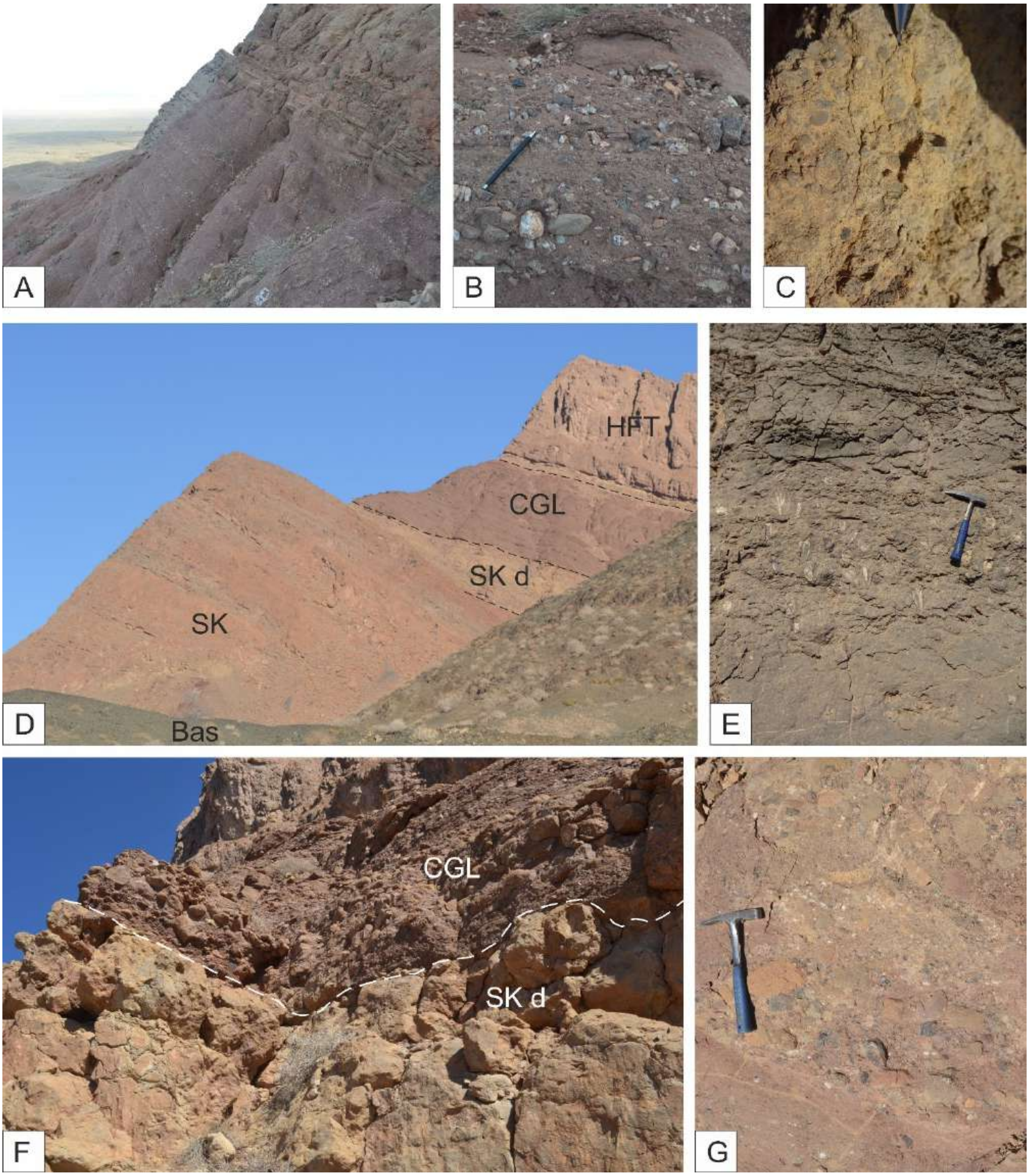

Fig. 6 – Lower part of the Cretaceous succession north of Arusan. A) Basal sandstone deposited above the metamorphic basement; B) detail of a sandy conglomerate mostly consisting of quartz pebbles; C) orbitolinid foraminifera in a limestone interval at the transition between sandstone and carbonate units; D) view of the lower part of the succession north of Khur (Bas: Basement; SK: Shah Kuh Formation; SKd: bedded limestone of the upper Shah Kuh Formation; CGL: Conglomerate; HFT: Haftoman Formation); E) rudists in life position in the massive part of the Shah Kuh Formation; F) base of the conglomeratic unit above the Shah Kuh Formation, with an evident erosional base; G) detail of the carbonate clasts in the conglomerates.

https://doi.org/10.1016/j.jseaes.2023.105736

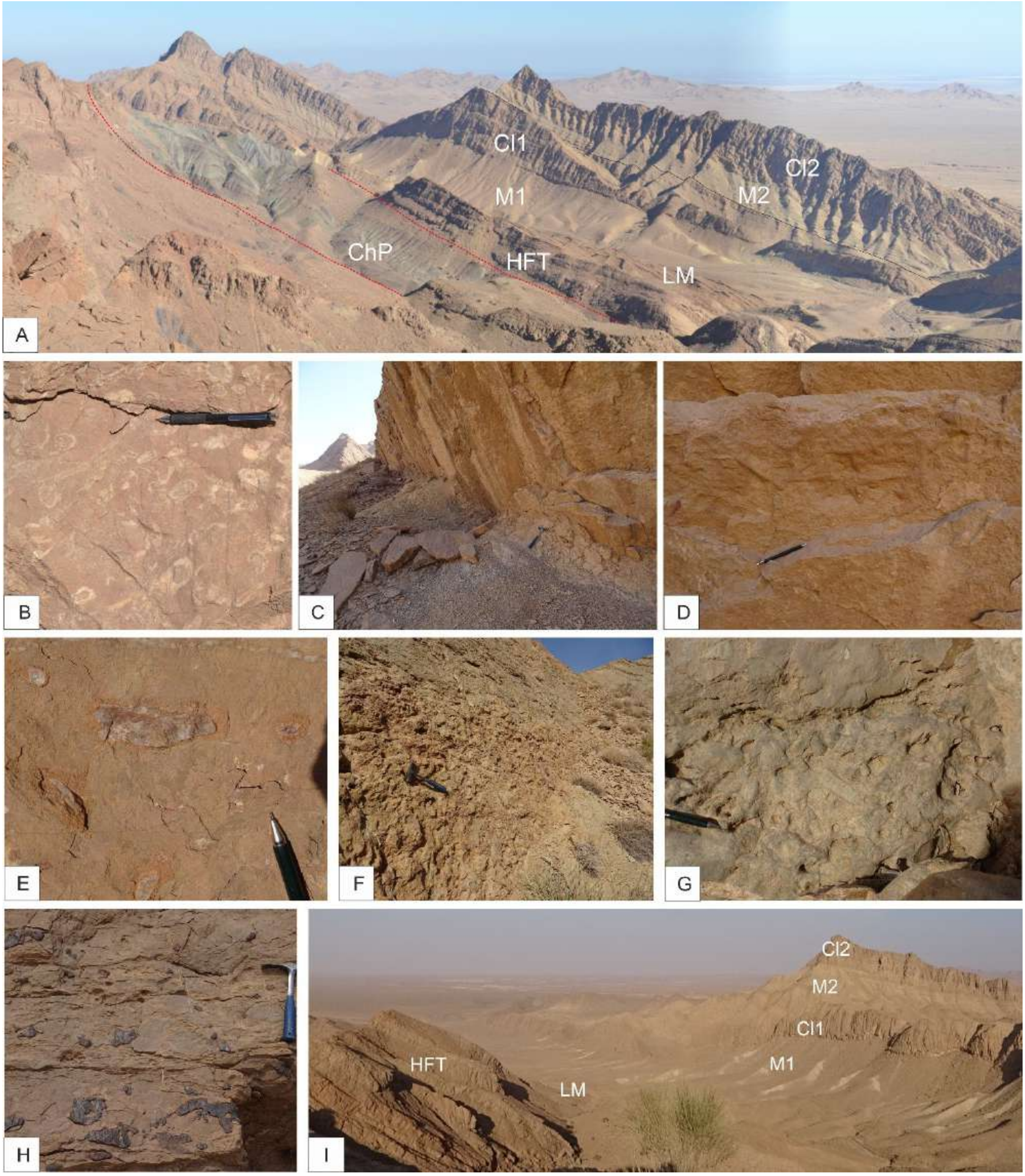

Fig. 7 – Upper part of the Cretaceous succession at Arusan. A) View of the succession south of a major fault separating the Chah Palang Formation from the Haftoman Formation and younger units; B) rudists in the Haftoman Formation; C) sharp boundary between M1, left, and CL1, right; D) detail of the base of CL1 with *Thalassinoides* bioturbations; E) chert nodules in CL1; F) hard ground at the top of top of CL1; G) detail of the hardground, with glauconite and abundant cephalopod shells; H) chert nodules in CL2; I) view of the succession. Abbreviations: ChP: Chah Palang Formation, HFT: Haftoman Formation; LM: Limestone and marls, upper part of the Haftoman Formation; M1: lower marls; CL1: lower cherty limestone; M2: upper marls; CL2: upper cherty limestone; from M1 to CL2: Farrokhi Formation.

https://doi.org/10.1016/j.jseaes.2023.105736

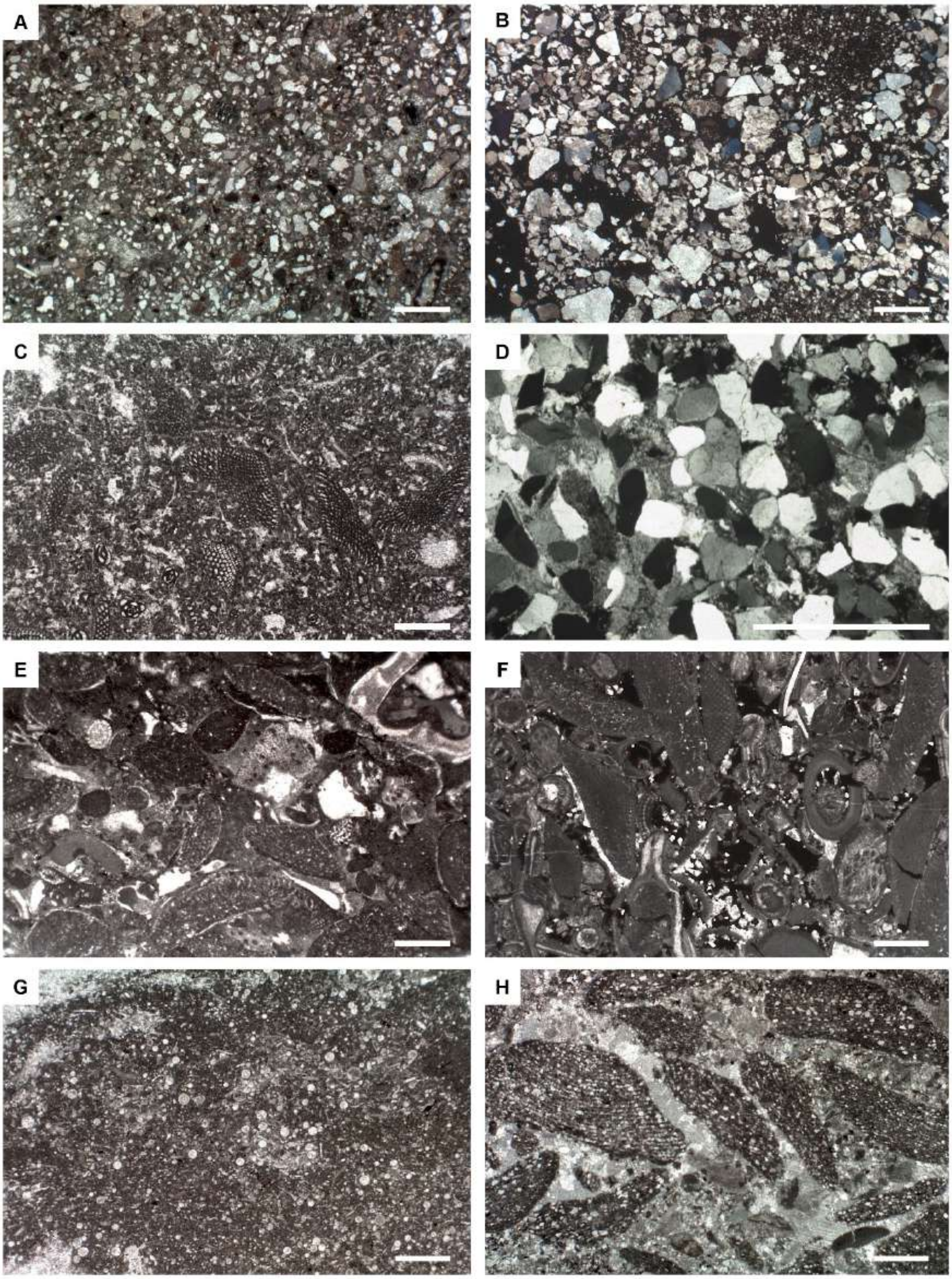

Fig. 8. Microfacies from the Arusan, Tiran, and Esfahan north areas - lower part of the successions. (A) Sandy limestone with silicic clasts. CSS, log K3, sample Ku28, (B) Sandstone with carbonate and silicic clasts. CSS, log Kalahrood, sample M3, (C) Orbitolinid-rich packstone with smaller benthic foraminifers. OBL, log K3, sample Ku29, (D) Well-sorted quartzarenite with prevailing monocrystalline grains; carbonate cements. QTZ, log K4, sample Ku31, (E) Orbitolinid-rich packstone with bryozoans and echinoid spines. OBL, log Tiran, sample CD71, (F) Orbitolinid-rich grainstone with echinoid spines, bryozoans, and coated grains showing interparticle and intraparticle porosity types. OBL, log Kalahrood, sample M22, (G) Packstone rich in radiolarians and sponge spiculae with planktonic foraminifers and pelagic pelecypods. CHL, log K4, sample Ku30, (H) Grainstone with orbitolinids incorporating abundant quartz micrograins. OBL, log K9, sample Ku144. Scale bar is 1 mm.

https://doi.org/10.1016/j.jseaes.2023.105736

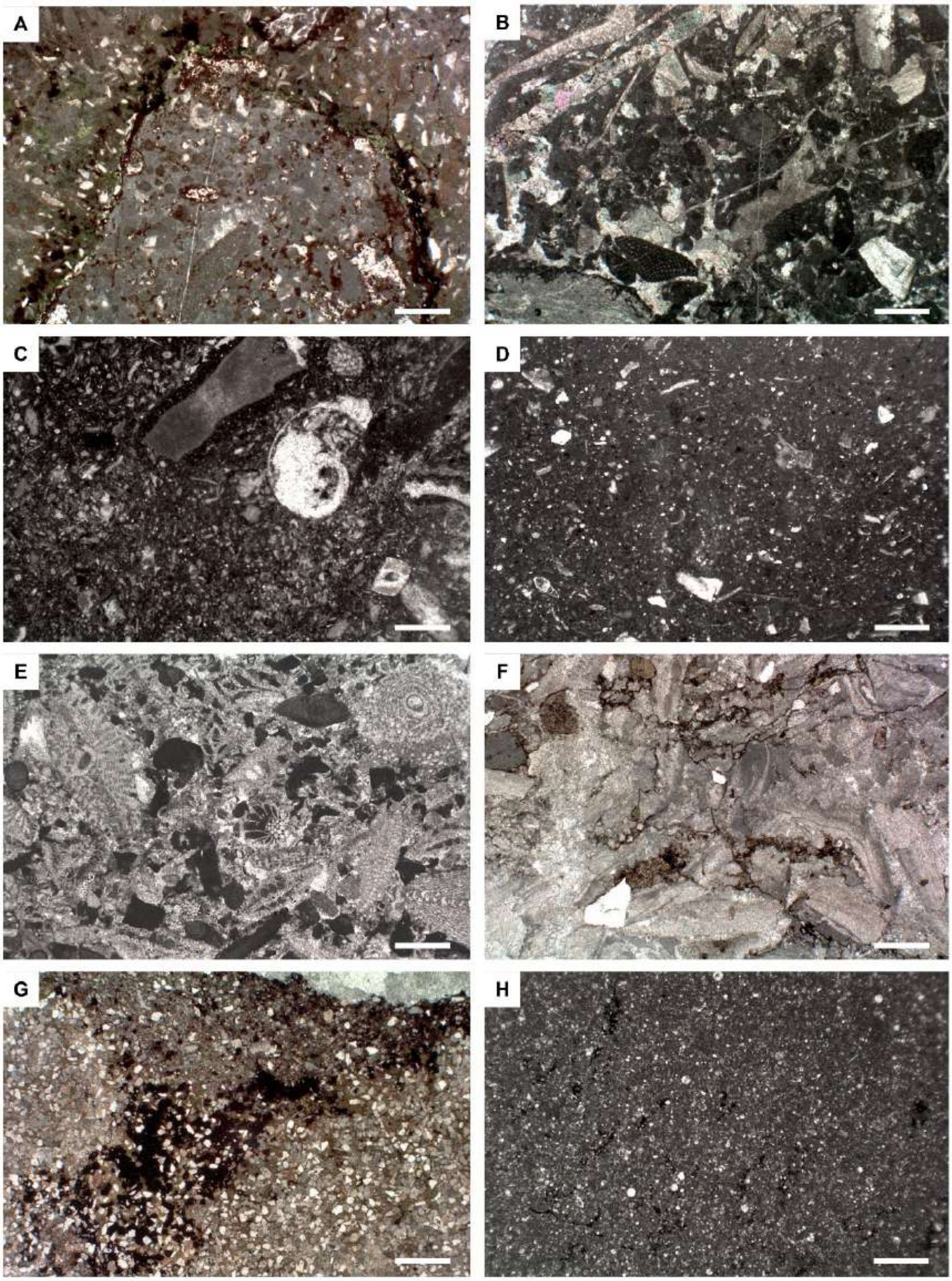

Fig. 9. Microfacies from the Arusan, Tiran, and Esfahan north areas - upper part of the successions. (A) Hardground within a skeletal packestone-wackestone. HGL, log Morgh, sample M51, (B) Packstone with orbitolinids, planktonic foraminifers, rudist fragments and peloids. OBE, log Morgh, sample M67, (C) Skeletal packstone with ammonoids, planktonic foraminifers and radiolarians. CHL, log Morgh, sample M60, (D) Wackestone with planktonic foraminifers, radiolarians, and sponge spiculae. MRL, log Kalahrood, sample M74bis, (E) Orbitoidid-rich grainstone with red algae. ODL, log K2, sample Ku19, (F) Skeletal packstone-grainstone with glauconite. HGL, log K9, sample Ku150, (G) Hardground within a sandy limestone with silicic clasts. HGL, log K9, sample Ku153b, (H) Packstone-wackestone with radiolarians, spongae spiculae, and rare planktonic foraminifers. CHL, log K0, sample Ku133. Scale bar is 1 mm.

https://doi.org/10.1016/j.jseaes.2023.105736

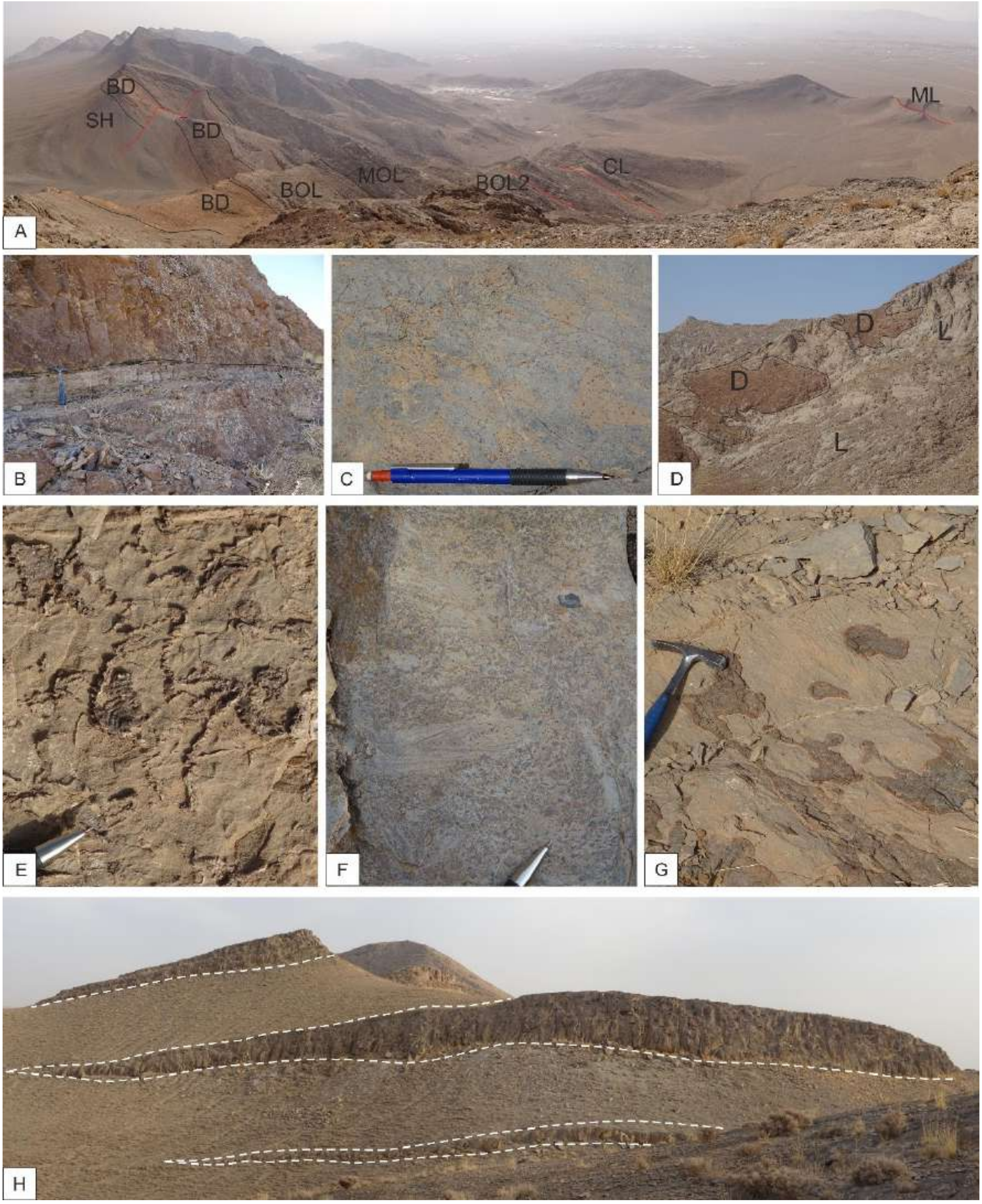

Fig. 10 – Stratigraphic succession at Tiran: A) General view (from NW) of the measured log, with the identification of the major units (SH: sandstone, equivalent to the Shemshak Group, BD: Basal dolostone; BOL: lower bedded Orbitolina limestone; MOL: Massive Orbitolina limestone; BOL2: upper bedded Orbitolina limestone; BD to BOL2 corresponding to the Shah Kuh Formation; CL: cherty limestone; ML: marls and limestone); B) sharp base of the marine carbonates above the quartz-rich sandstone; C) bioturbated Orbitolina wackestone; D) view of the patchy dolomitization (D) within the massive limestone (L) of the lower part of the Cretaceous succession; E) silicified bivalves on the bedding surface (resembling *Rastellum carinatum* Lamark); F) resedimented Orbitolina-rich limestone; G) chert nodules in the limestone intercalated with marls; H) view of the upper part of the log, with lenticular limestone, rich in orbitolinids and ostreids, intercalated in a the marly succession.

https://doi.org/10.1016/j.jseaes.2023.105736

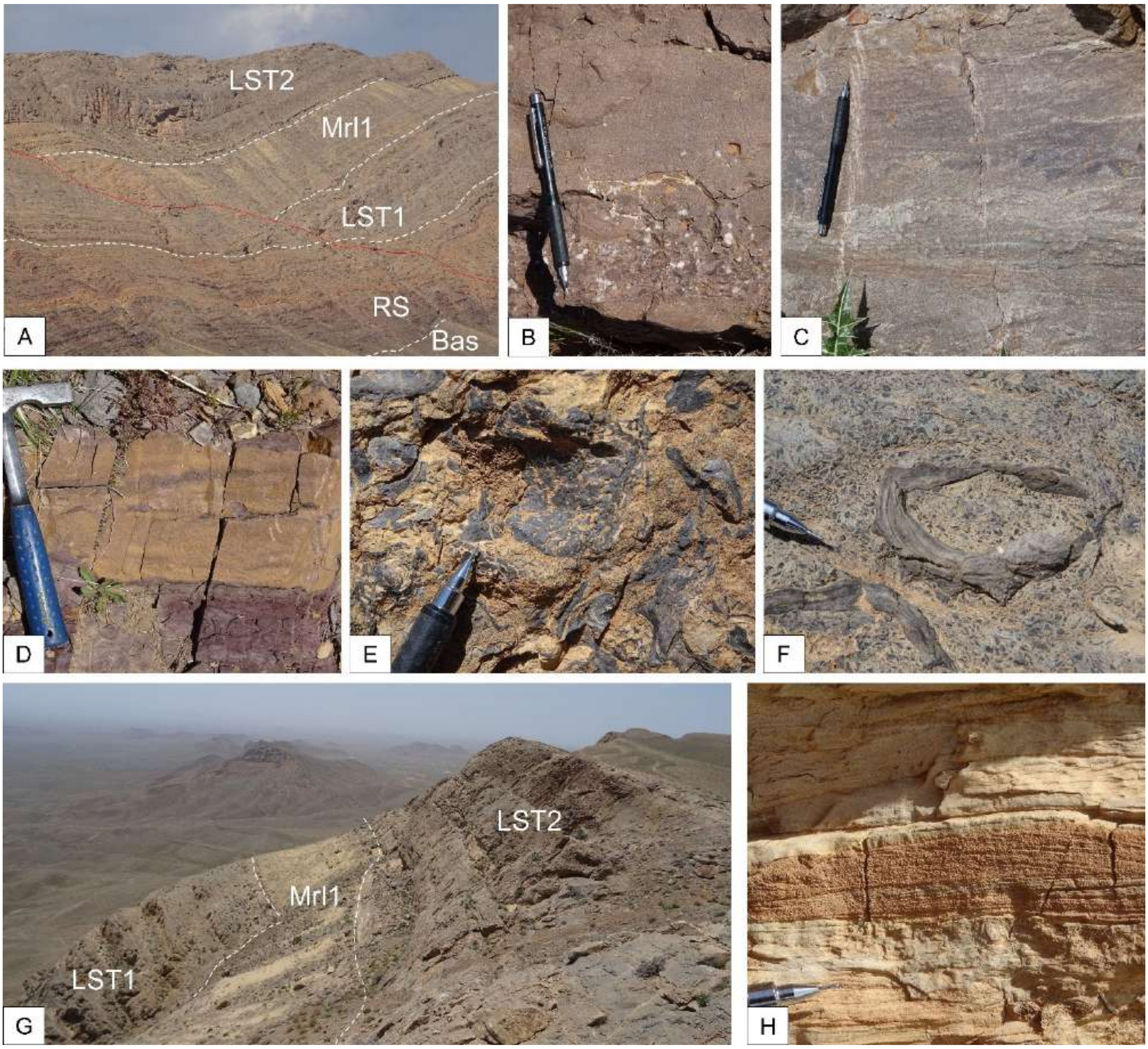

Fig. 11 – Cretaceous succession at Morgh (Esfahan north). A) View of the Cretaceous succession covering slightly metamorphic quartzarenites and conglomerates (Bas: basement; RS: red sandstone with carbonate cement; LST1: first limestone interval; Mrl1: lower marly interval; LST2: main limestone unit, possibly Taft Formation); B) quartz-rich conglomerate at the base of the Cretaceous succession (equivalent of the Noqreh Formation); C) cross-laminated quartzarenite bed; D) hybrid limestone, with quartz grains and cross laminations, documenting the first marine conditions in the Cretaceous succession; E) sandy limestone with large bivalves (ostreids) with evidence of intense bioerosion; F) bioclastic rudstone with ostreids and orbitolinids, at the transition between RS and LST1; G) Upper part of the Cretaceous succession, with the marly interval (Mrl1) between the two main carbonate units (LST1 and LST2); H) cross-laminated sandy limestone at the base of LST2.

https://doi.org/10.1016/j.jseaes.2023.105736

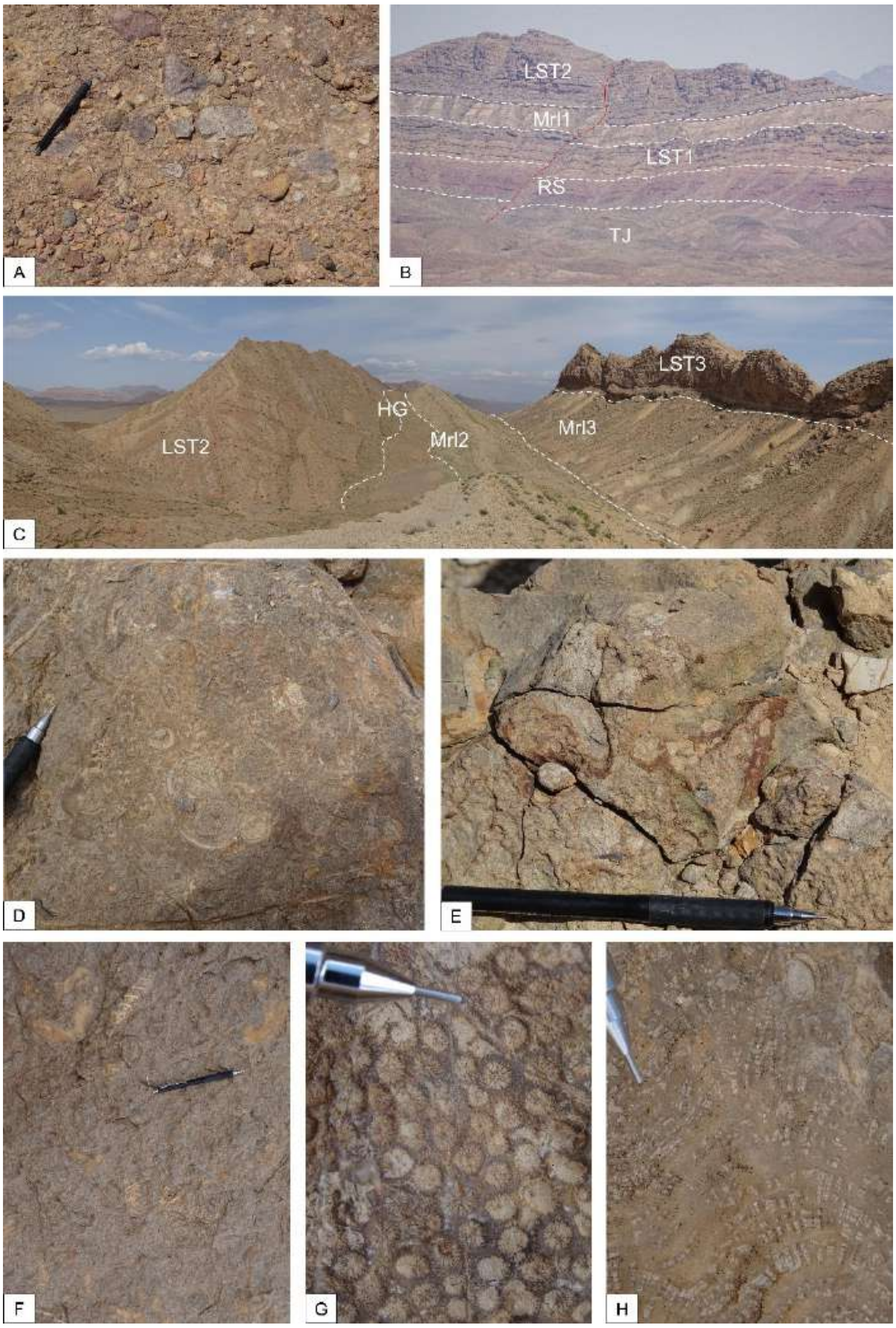

Fig. 12 – Cretaceous succession at Kalahrood (Esfahan north). A) conglomerate with quartz pebbles at the base of the Cretaceous succession, resting upon a Triassic to Jurassic tilted mixed siliciclastic-calcareous succession; B) View of the lower part of the Cretaceous succession (TJ: Triassic to Jurassic tilted mixed siliciclastic-calcareous succession; RS: red sandstone with carbonate cement; LST1: first limestone interval; Mrl1: lower marly interval; LST2: main limestone unit (Shah Kuh Formation?); HG: hard ground at the top; Mrl2: marl to marly limestone interval with ammonoids and pelagic foraminifera; Mrl3: marls; LST3: prograding bioclastic limestone unit); C) upper part of the Cretaceous succession; D) rudists in life-position in the massive limestone of unit LST2; E) detail of the hard-ground at the top of LST2, with glauconitic grains and Fe-rich crusts; F) large gastropods (nerineids) in a bioclastic rudstone with corals and stromatoporoids, Unit LST3; G) detail of a coral colony in Unit LST3; H) stromatoporoid in Unit LST3. Abbreviations: TJ: Triassic to Jurassic tilted mixed siliciclastic-calcareous succession; RS: red sandstone with carbonate cement; LST1: first limestone interval; Mrl1: lower marly interval; LST2: main limestone unit (Shah Kuh Formation?); HG: hard ground at the top; Mrl2: marl to marly limestone interval with ammonoids and pelagic foraminifera; Mrl3: marls; LST3: prograding bioclastic limestone unit.

https://doi.org/10.1016/j.jseaes.2023.105736

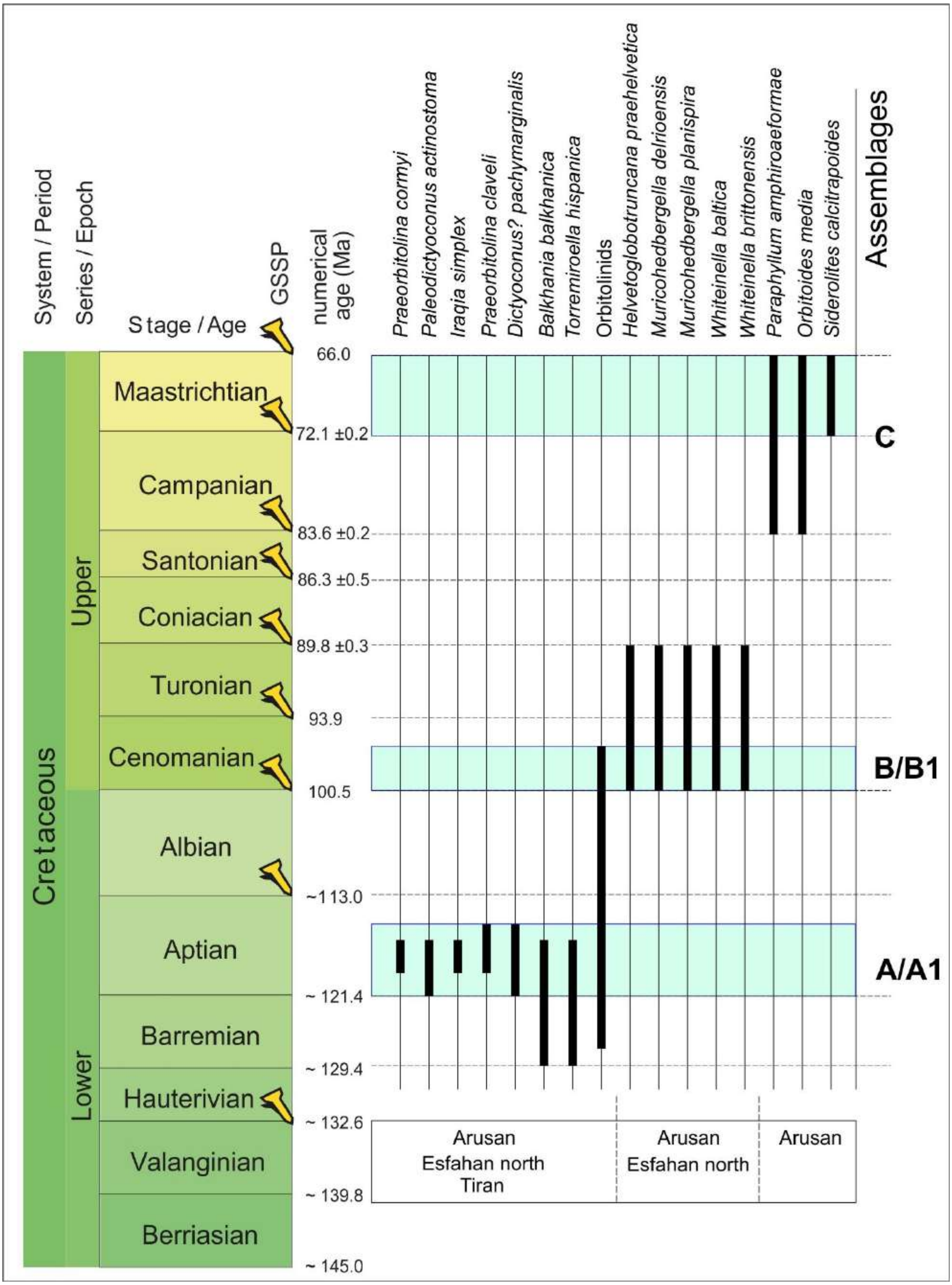

Fig. 13 - Distribution chart of the foraminifera occurring in the three studied areas identifying the assemblages used to constrain the age of the successions.

https://doi.org/10.1016/j.jseaes.2023.105736

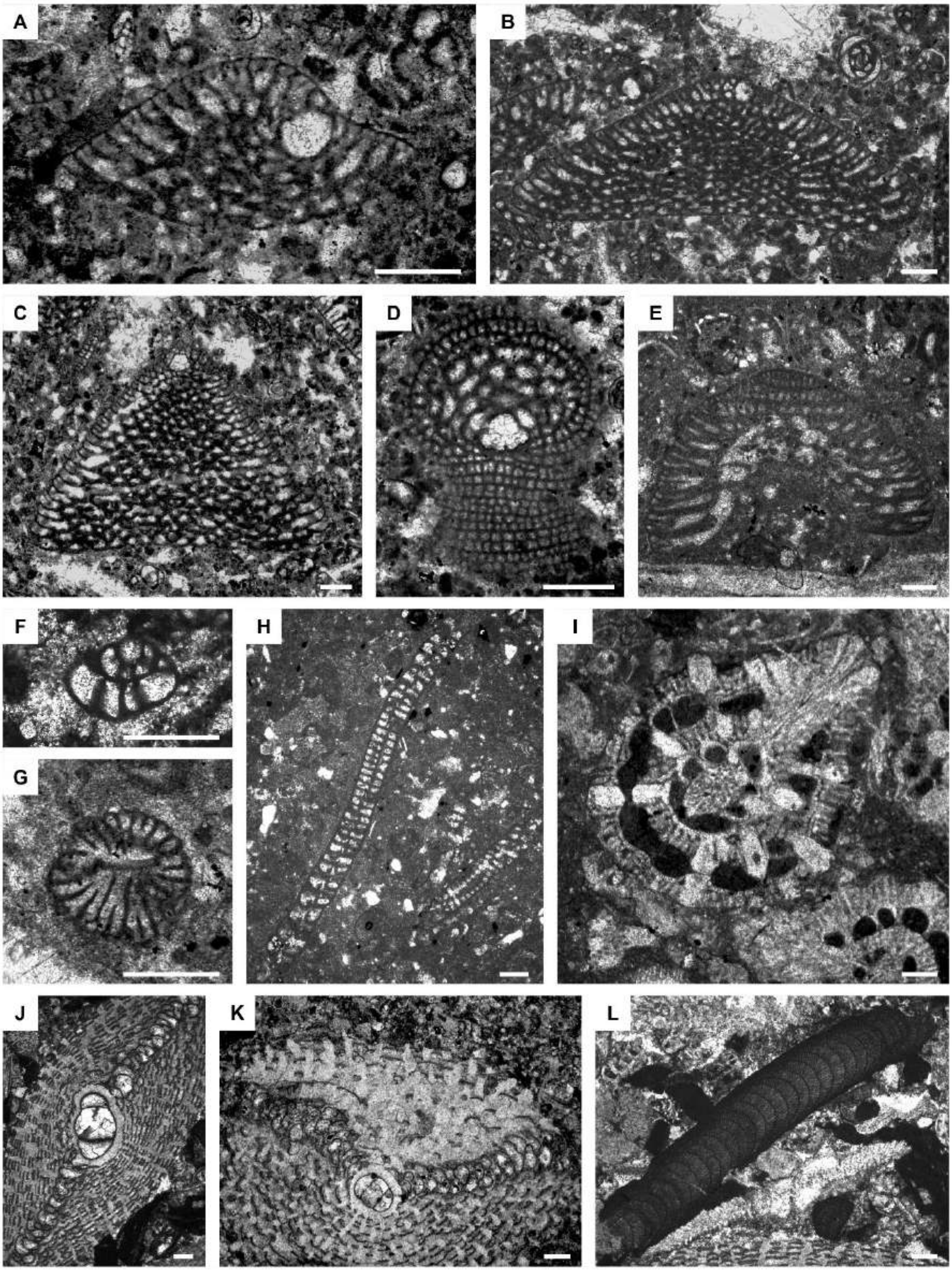

Fig. 14. Arusan area microfossil assemblage. (A) *Praeorbitolina cormiy* Schroeder, log K3, sample Ku29, (B) *Palaeodictyoconus* cf. *actinostoma* Arnaud-Vanneau and Schroeder, log K3, sample Ku29, (C) Orbitolinid indet., log K3, sample Ku 29, (D) *Praeorbitolina* aff. *claveli* Schlagintweit et al., log K3, sample Ku29, (E) *Dictyoconus*? *pachymarginalis* Schroeder, log K0, sample Ku105, (F) *Nezzazata isabellae* Arnaud-Vanneau and Sliter, log K0, sample Ku105, (G) *Akcaya minuta* (Hofker), log K0, sample Ku105, (H) *Cuneolina* cf. *hensoni* Dalbiez, log K1, sample Ku3, (I) *Siderolites calcitrapoides* Lamarck, log K9, sample Ku157, (J, K) *Orbitoides media* (D'Archiac), log K0, sample Ku122, Ku123, (L) *Paraphyllum amphiroaeformae* (Rothpletz), log K2 sample Ku19. Scale bar is 200 µm.

https://doi.org/10.1016/j.jseaes.2023.105736

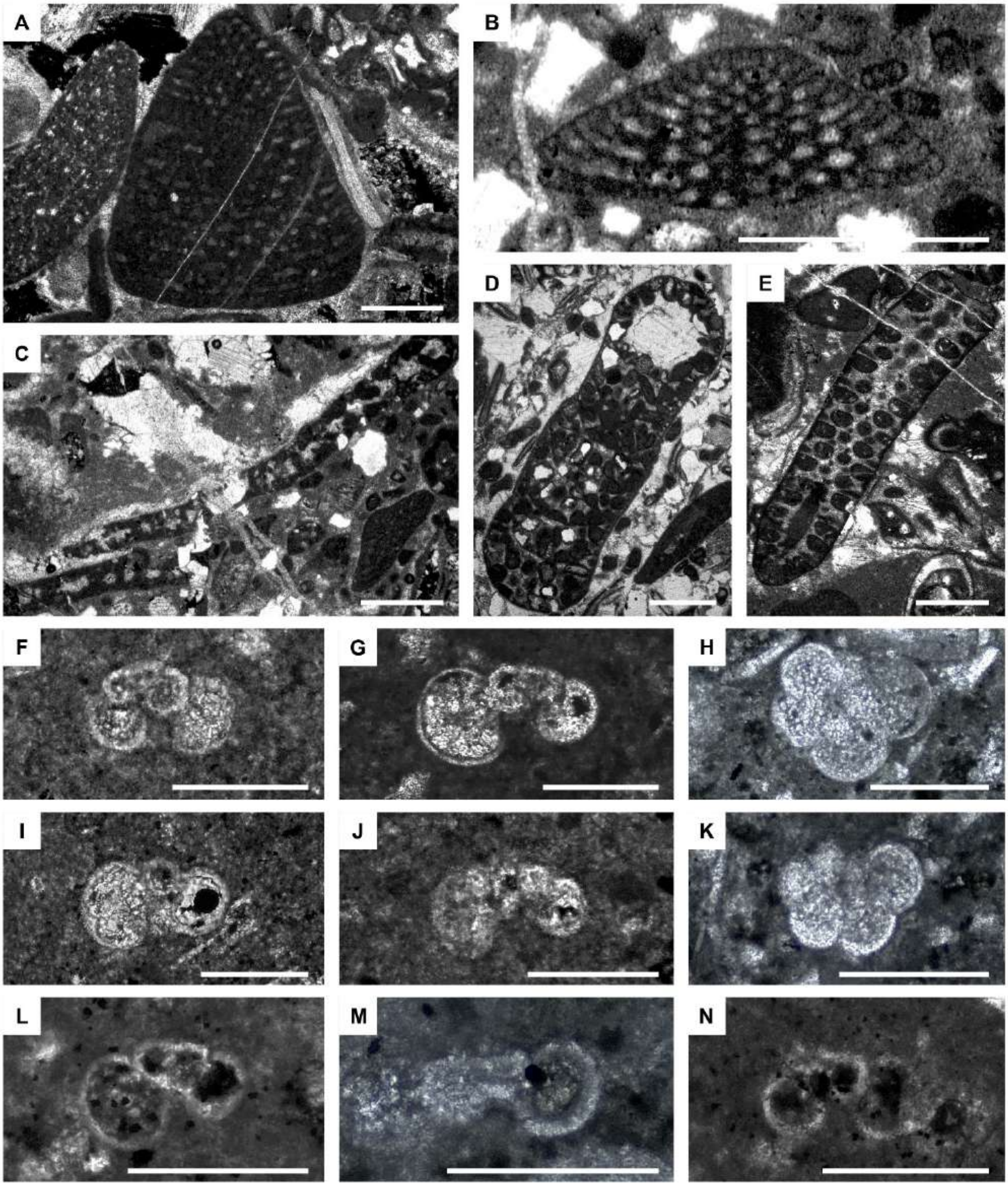

Fig. 15 - Esfahan north area assemblage. (A) *Iraqia* cf. *simplex* Henson, log Kalahrood, sample M12, (B) Orbitolinid indet., log Morgh, sample M33, (C) *Balkhania balkhanica* Mamontova, log Morgh, sample M33, (D) *Torremiroella hispanica* Brun and Canérot, log Morgh, sample M36, (E) *Bakalovaella elitzae* (Bakalova), log Kalahrood, sample M15, (F, G) *Whiteinella brittonensis* (Loeblich and Tappan), log Morgh, samples M50, M74bis, (H, I) *Whiteinella baltica* Douglas and Rankin, samples M60, M74bis, (J) *Helvetoglobotruncana praehelvetica* (Trujillo), log Morgh, sample M50, (K, L) *Muricohedbergella delrioensis* (Carsey), log Morgh, log Morgh, samples M60, log Kalahrood, M74bis (M, N) *Muricohedbergella planispira* (Tappan), samples M56, M74bis. Scale bar is 200 µm.

https://doi.org/10.1016/j.jseaes.2023.105736

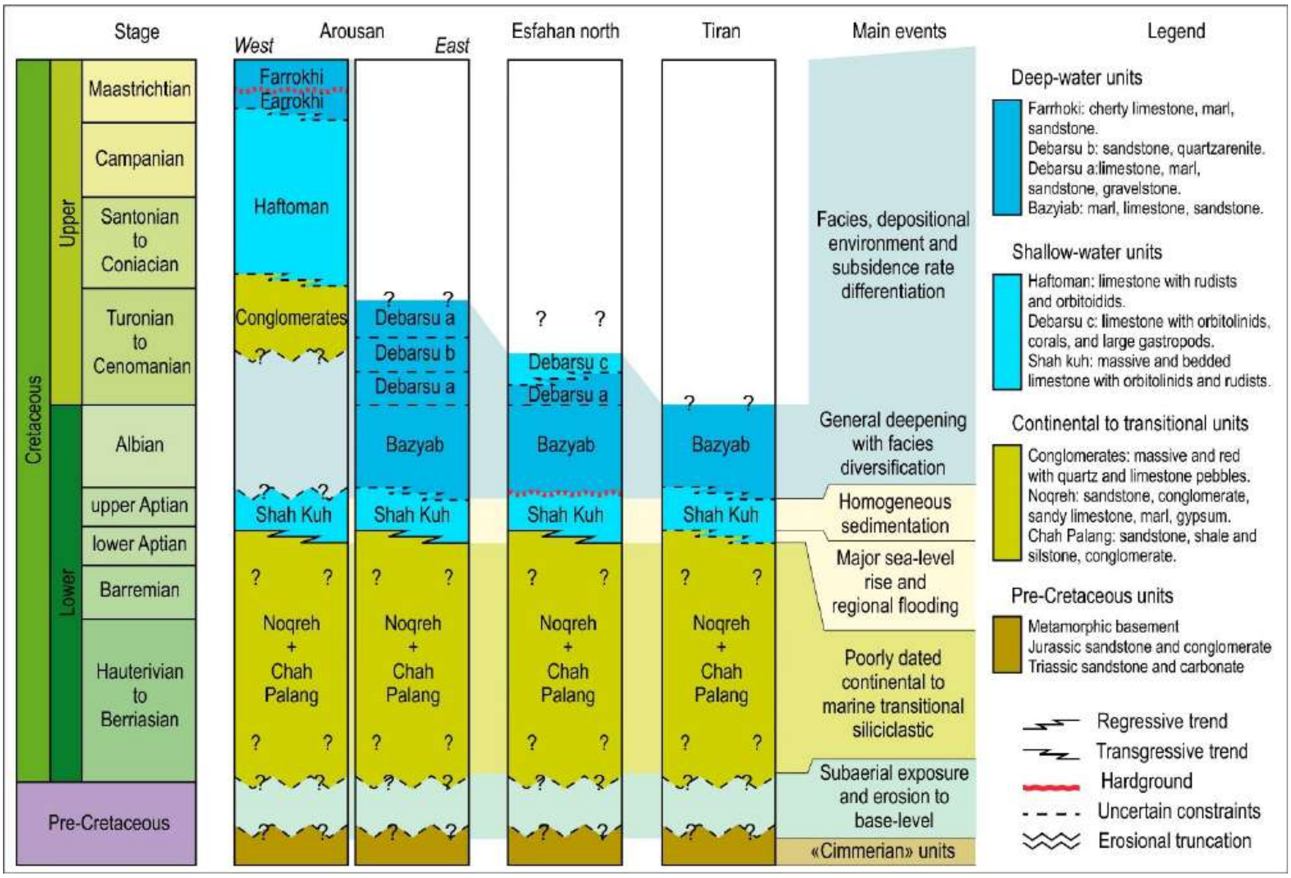

Fig. 16 – Comparison of the stratigraphic evolution of the three studied areas, with the identification of the major intervals marking possible eustatic and tectonic events.

Code name	Facies	Main features	Main constituents	Environmental interpretation	Locality
CSS	conglomerate, sandstone, and siltstone	poorly bedded, faint cross laminations, reddish colour, dolomitized matrix and carbonate cement	quartz, lithics	Coastal siciliclastic	Arusan, Tiran, Esfahan N
HYB	hybrid packstone with dispersed pebbles	bedded hybrid limestone, rare laminations	quartz, lithics, orbitolinids and rudists	Proximal epeiric platform with siliciclastic input	Arusan, Tiran
RLM	packstone and wackestone	poorly bedded, dolomitized matrix	rudists, bryozoans, bioclasts, benthic foraminifers, quartz, lithics	Epeiric carbonate platform with siliciclastic input	Arusan, Tiran, Esfahan N
OBL	packstone and grainstone	massive or lenticular geometries	echinoderms, dasycladacean algae, orbitolinids, crinoids, rudists, ostreids, quartz, lithics	A) Proximal epeiric carbonate platform with siliciclastic input; B) resedimented limestone in basinal settings	Arusan, Tiran, Esfahan N
ODL	grainstone and packstone	well-bedded to massive limestone	crinoids, orbitoidids, red algae, rudists, ostreids	A) High energy epeiric carbonate platform; B) resedimented limestone in basinal settings	Arusan
CHL	wackestone and packstone	well-bedded, bioturbations, chert nodules	echinoderms, brachiopods, planktonic foraminifera, radiolarians, calcisphaeres, pelagic pelecypods, sponge spiculae, quartz, lithics	Basinal setting below storm wave base	Arusan, Tiran, Esfahan N
HGL	packstone	hardground, glauconitic crusts	ammonites, belemnites, gastropods, echinoids, and bivalves	Basinal setting below storm wave base	Arusan, Esfahan N
OBE	packstone to rudstone	Massive to poorly-bedded limestone	rudists, gastropods, corals, stromatoporoids, orbitolinids, rare planktonic foraminifers	Epeiric carbonate platform with siliciclastic input	Esfahan N
MRL	marl and siltstone	massive to bedded marl and siltstone, gray to greenish, bioturbations	radiolarians, ammonites, sponge spiculae, echinoids	Basinal setting below storm wave base	Arusan, Tiran, Esfahan N
CGL	conglomerate with carbonate pebbles	massive to amalgamated beds	rounded carbonate and rare basement pebbles	Coastal siciliclastic	Arusan
QTZ	quartzarenite	cross and parallel laminated, bioturbated quartzarenite with carbonate cement	rare fragments of echinoids, glaucony	Basinal setting below storm wave base	Arusan

Tab. 1 - description and components of the main facies reconstructed by the integration of fiend and microscopic observations.

https://doi.org/10.1016/j.jseaes.2023.105736

Units	Arusan W	Arusan E	Esfahan N	Tiran
Farrokhi Fm				
Haftoman Fm	RLM, ODL			
Conglomerates	CGL			
Debarsu c			OBE, RLM	
Debarsu b		QTZ		
Debarsu a		MRL	MRL, CHL	
Bazyab Fm		MRL	MRL, HGL	MRL, CHL
Shah Kuh Fm	RLM, OBL, HYB	RLM, OBL, HYB	RLM, OBL, HYB	RLM, OBL
Noqreh Fm + Cha Palang Fm	CSS, HYB	CSS, HYB	CSS, HYB	CSS, HYB

Tab. 2 – Associations of the different facies types recognized (Tab. 1) in the different units present in the studied sections. The nomenclature of the units is the same of that used in Fig. 16

https://doi.org/10.1016/j.jseaes.2023.105736